

multi-Risk sciEnce for resilienT commUnities undeR a changiNgclimate

Codice progetto MUR: **PE00000005** – C93C22005160002



Deliverable title: Adaptive modelling of scenarios through increasing inclusion of protection and mitigation

Deliverable ID: 1.4.6

Due date: 01/12/2024

Submission date: 01/12/2024

AUTHORS

**Andrea D'Alpaos (UNIPD), Alice Puppini (UNIPD), Alvisio Finotello (UNIPD),
Agnese Baldoni (UNIVPM)**

Technical references

Project Acronym	RETURN
Project Title	multi-Risk sciEnce for resilienT commUnities undeR a changiNg climate
Project Coordinator	Domenico Calcaterra UNIVERSITA DEGLI STUDI DI NAPOLI FEDERICO II domcalca@unina.it
Project Duration	December 2022 – November 2025 (36 months)
Deliverable No.	DV1.4.6
Dissemination level*	
Work Package	W1.P4 - Coastal flooding and beach erosion under environmental and climatic changes
Task	1.4.3 – Coastal floods and beach erosion impact modelling
Lead beneficiary	UNIPD
Contributing beneficiary/ies	Andrea D'Alpaos (UNIPD), Alice Puppini (UNIPD), Alvise Finotello (UNIPD), Agnese Baldoni (UNIVPM)

* PU = Public

PP = Restricted to other programme participants (including the Commission Services)

RE = Restricted to a group specified by the consortium (including the Commission Services)

CO = Confidential, only for members of the consortium (including the Commission Services)

Document history

Version	Date	Lead contributor	Description
0.0	01/10/2024	Andrea D'Alpaos, Alice Puppini, Alvise Finotello	First draft
1.0	10/11/2024	Alice Puppini, Alvise Finotello, Agnese Baldoni	Second draft
2.0	2/12/2024	Andrea D'Alpaos, Alice Puppini, Alvise Finotello	Final draft

ABSTRACT

Coastal areas, critical to human development and economic activity, face increasing pressures from climate change-driven hazards such as flooding and erosion. Traditional hard engineering solutions for coastal protection are proving inadequate to manage escalating risks, prompting a shift toward Nature-based Solutions (NbS). These approaches leverage natural ecosystems to mitigate risks while providing co-benefits such as carbon sequestration, biodiversity enhancement, and socio-economic opportunities. This report evaluates the potential of nature-based strategies in coastal risk management, providing insights from specific case studies.

The report explores the management and restoration of salt marshes and seagrass meadows in the Venice Lagoon, assessing their role in enhancing ecosystem resilience and delivering bio-morphodynamic and carbon sequestration co-benefits. It examines the protective capacity of oyster and polychaete reefs in reducing beach erosion and flooding, showcasing hybrid NbS that integrate natural and engineered approaches. The adaptation of coastal defense structures in the Misa River estuarine system is also analyzed to highlight the potential of NbS to enhance flood resilience while maintaining ecological functionality.

Findings demonstrate the versatility of NbS as sustainable alternatives to conventional coastal defense strategies. While the adoption of NbS in the Mediterranean region remains limited due to knowledge gaps and regulatory challenges, these solutions hold significant promise for fostering resilient and sustainable coastal communities. To scale up NbS implementation, greater investment in cross-sectoral collaboration, research, and policy development is essential. This report provides valuable insights into the design, application, and benefits of NbS, offering a framework for advancing adaptive coastal management in the face of climate change.

Table of contents

1. Introduction	8
2. Management and restoration of salt marshes and seagrass meadows in the Venice Lagoon	10
2.1. Large-scale restoration under the Venice Special law	11
2.2. Life Natura salt marsh protection and restoration through natural engineering techniques at Palude dei Laghi	11
2.3. Life Vimine salt marsh soil-bioengineering	12
2.4. Life Lagoon Refresh: restoration of a brackish marsh environment	13
2.5. Seagrass transplantation initiatives	13
3. Exploring morphodynamic co-benefits of salt-marsh restoration: insights from the Venice Lagoon (Italy)	15
3.1. Introduction	15
3.2. Materials and Methods	16
3.2.1. Geomorphological setting	16
3.2.2. Salt marshes in the Venice lagoon: current state	19
3.2.3. Numerical modeling	20
3.2.4. Numerical simulations	24
3.3. Results and Discussion	26
3.3.1. Water levels	26
3.3.2. Significant wind-wave heights	26
3.3.3. Bed shear stresses	27
3.3.4. Sediment budget at the Lagoon scale	28
3.4. Conclusions	30
4. Carbon sequestration potential of salt marsh restoration: insights from the Venice Lagoon Case Study	31
4.1. Methods	31
4.2. Results	32
5. Adaptation of coastal defense structures against coastal flooding in the Misa River estuarine system	34
5.1. Methods	34
5.2. Results	35
References	38

Figures

Figure 1. Examples of fascines produced locally (upper left) and then placed to protect salt marsh edges from erosion in LIFE VIMINE (Barausse et al., 2015).....	13
Figure 2. Seagrass transplantation sites in the LIFE SeResto project (green) and monitoring sites (red) (Bonometto et al., 2018).	14
Figure 3: Geomorphological Setting. (a) The Venice Lagoon captured in satellite imagery (Copernicus Sentinel, 2020). Natural salt marshes are outlined in yellow, while restored salt marshes are depicted in purple. (b, c, d) Detailed views of the three primary lagoon inlets. (e) A rose-diagram illustrating the wind climate data recorded at the "Chioggia Diga Sud" anemometric station from 2000 to 2019. Notably, it highlights the two predominant winds: the north-easterly Bora wind and the south-easterly Sirocco wind. (Image © Finotello et al., 2023).	17
Figure 4: Morphological evolution of the Venice lagoon based on available historical bathymetric maps; (from top) 1901, 1932, 2003. (L. D'Alpaos, 2010)	18
Figure 5: Google Earth photo showing artificial salt marshes in the southern Venice lagoon near Chioggia.....	20
Figure 6: Marsh restoration using nature-based solution (https://www.lifevimine.eu).....	20
Figure 7: The data used in the numerical simulations pertain to a specific time period from November 17, 2005, to December 17, 2005. Water levels were monitored and recorded at the "CNR Oceanographic Platform," and wind data were collected from the "Chioggia Diga Sud" anemometric station, as depicted in panel (b). The computational grid employed in the numerical model is illustrated in panel (b) and corresponds to the 2014 morphological configuration of the Venice Lagoon. Panels (c) and (d) compare the distributions of water levels (c) and wind climate (d) during the analyzed period to those observed over the period from 2000 to 2019, represented in grey. These comparisons provide valuable context for understanding the conditions simulated in the study. (Image from Finotello et al., 2023)	25
Figure 8: Differences in numerically modeled maximum water levels across the Venice lagoon. Results are presented as maps of differential values between the 2014 (i.e., present-day) configuration of the Venice lagoon and other morphological configurations. A) Differences between 2014 and 1901; B) Differences between 2014 and 1932; C) Differences between 2014 and the "Restored 1901" scenario; D) Differences between the 2014 and "Restored 1932" scenario. Note different colormap scales for panels A-B and C-D.	26
Figure 9: Differences in numerically modeled significant wave heights across the Venice lagoon. Results are presented as maps of differential values between the 2014 (i.e., present-day) configuration of the Venice lagoon and other morphological configurations. A) Differences between 2014 and 1901; B) Differences between 2014 and 1932; C) Differences between 2014 and the "Restored 1901" scenario; D) Differences between the 2014 and "Restored 1932" scenario. Note different colormap scales for panels A-B and C-D.	27
Figure 10: Differences in numerically modeled maximum bed shear stresses across the Venice lagoon. Results are presented as maps of differential values between the 2014 (i.e., present-day) configuration of the Venice lagoon and other morphological configurations. A) Differences between 2014 and 1901; B) Differences between 2014 and 1932; C) Differences between 2014 and the "Restored 1901" scenario; D) Differences between the 2014 and "Restored 1932" scenario. Note different colormap scales for panels A-B and C-D.	28
Figure 11: Modeled changes in sediment volumes across different morphological units are presented. For salt marshes, tidal flats, and tidal channels, positive values indicate sediment deposition, while negative values represent erosion. For inlets, sediment volumes are calculated as the integral of sediment flux across all lagoonal inlets, where positive values	

denote sediment import into the lagoon and negative values represent sediment export to the open sea. 29

Figure 12: Modelled salt-marsh vertical accretion rates (taken here as the vertical accretion due to mineral sediment deposition alone) for different morphological configurations of the Venice Lagoon. 29

Figure 13. Carbon accumulation and CO₂ sequestration estimate in the salt marshes of the Venice Lagoon (modified from Puppini et al., 2024). 33

Figure 15. Results of the semi-analytical model by Marini et al. (2022), showing the non-dimensional beach profile recession ΔYH_0 depending on the breakwater freeboard R_c 35

Figure 16. Map of the differences in water depths in the flooded areas behind the breakwaters. The difference was computed between the simulations run with i) original breakwaters and ii) adapted breakwaters. 36

Figure 17. Map of the mean water levels at the sixth hour of the simulations (peak of the simulated storm) run with original breakwaters (left) and adapted breakwaters (right). 36

Figure 18. Map of the maximum wave height at the sixth hour of the simulations (peak of the simulated storm) run with original breakwaters (left) and adapted breakwaters (right). 37

1. Introduction

Coastal areas are essential to human development, offering numerous **economic and social benefits**. As a result, a significant portion of human settlements are located along coastlines, hosting a share of the global population that has been increasing rapidly over the last decades (Neumann et al., 2015). Estimates indicate that at least **10% of the world's population** currently lives in coastal areas lying less than **10 meters above the mean sea level** (McGranahan et al., 2007; Merkens et al., 2016), and roughly **one-third of the European Union's population** resides within **50 kilometers of the coast**.

Thus, **coastal zones** play a critical role in **territorial structuring and development** and are typically characterized by **rapid urbanization, high population density, seasonal tourism**, and often **conflicting economic interests**. These dynamics increase pressure on these sensitive and vulnerable zones (IPCC, 2014), where climate change-driven hazards, such as **flooding and extreme coastal erosion**, are increasingly causing significant **economic and social damage**. This trend underscores the need for prompt **risk mitigation and damage prevention through suitable adaptation strategies**.

Historically, **coastal protection** has relied on conventional "hard" engineering infrastructures, such as **seawalls, groins, sloping structures**, and **offshore barriers**. However, the growing recognition that these infrastructure-based solutions are insufficient to manage the **escalating risks** associated with climate changes (Pranzini et al., 2015) has led to a demand for more **flexible, cost-effective, resilient, and environmentally sustainable** measures (Eggermont et al., 2015).

Among the most promising modern approaches to coastal protection are **Nature-based Solutions (NbS)** (Gómez Martín et al., 2020). The **European Commission** defines NbS as "living solutions inspired by, continuously supported by, and using nature to address various societal challenges in a resource-efficient and adaptable manner, while also providing economic, social, and environmental benefits" (European Commission, Directorate-General for Research and Innovation, 2022). These solutions emphasize **biodiversity**, and the essential functions and processes of ecosystems, as part of holistic **climate adaptation strategies** (Gómez Martín et al., 2020).

As an umbrella concept, NbS encompass diverse **conservation and sustainability measures**. Terms like **green infrastructure, ecosystem-based adaptation, ecosystem-based mitigation, hybrid infrastructure, ecosystem restoration**, and **ecosystem protection** all fall within the NbS framework. One of their key advantages over traditional adaptation strategies is their ability to generate **multiple co-benefits**. For instance, restoring or protecting **coastal wetlands** can enhance resilience to storms by acting as natural barriers. At the same time, these actions provide additional benefits like **carbon sequestration, biodiversity enhancement, fisheries resources, job creation**, and **tourism opportunities** (Woodward and Wui, 2001; Clarkson et al., 2014).

NbS are categorized into **three types** based on the level of **human intervention** (Zanin et al., 2024; Gómez Martín et al., 2020):

- **Type 1: Low human intervention** – These approaches focus on preserving the ecological integrity and stability of essential ecosystem functions and habitats without intensive management or interference. Examples include **ecosystem protection and conservation**.
- **Type 2: Medium human intervention** – This category includes management approaches that sustainably and multifunctionally enhance key ecosystem services. Examples include **ecosystem restoration** and management practices in **agricultural lands, forests, river systems, grasslands, and pastures**.

- **Type 3: High human intervention and hybrid solutions** – These approaches involve significant ecosystem modification or the creation of new ecosystems designed for multiple purposes. It includes **green (or blue, in aquatic ecosystems) infrastructures**, described by the **European Commission (2013)** as “a strategically planned network of natural and semi-natural areas designed to provide a wide range of ecosystem services.” Combining natural and grey infrastructure in **hybrid solutions** sometimes results in creating entirely new ecosystems.

This categorization underscores the versatility of **Nature-based Solutions** as a multi-benefit strategy. By aligning with sustainability principles, NbS offer a **dynamic approach to climate adaptation**, particularly in vulnerable coastal regions, where their ability to balance ecological health with human needs is critical.

Diverse habitats based on plant and animal formations, such as mangroves, salt marshes, seagrasses, beach dunes, coral reefs, oyster reefs, and polychaete reefs, provide natural coastal defense, primarily through wave reduction and sediment stabilization. As a result, the conservation, restoration, or even creation of these coastal ecosystems can significantly reduce the vulnerability of eroding coasts to current and projected increases in flooding, offering numerous benefits to the social-ecological system (Gómez Martín et al., 2020).

Zanin et al. (2024) reviewed the **adoption of NbS for coastal risk management in the Mediterranean** by analyzing 162 scientific papers and documents. Of these, only 23 were deemed relevant to the study, and **11 cases of NbS adoption** were identified. Among these, only one NbS was classified as 'Low human intervention' (seagrass conservation), six as 'Medium human intervention' (seagrass restoration, dune restoration, beach nourishment, restoration of sediment delivery, wetland restoration, and forest restoration), and four as 'High human intervention' (infrastructural drainage systems, coastal barriers, stone wall terraces, and dune construction).

Addressing the challenges posed by climate change and human pressures on coastal areas requires a paradigm shift from traditional hard engineering solutions to adaptive and sustainable approaches. NbS emerge as a promising alternative, integrating environmental conservation with climate adaptation and socio-economic benefits. However, their widespread adoption faces significant barriers, including knowledge gaps, regulatory hurdles, and limited financing.

To overcome these challenges, **greater awareness, cross-sectoral collaboration, and investments in research and policy development are essential**. Scaling up the application of NbS can enhance coastal resilience by helping communities adapt to climate change while preserving vital ecosystem services. The Mediterranean example highlights the potential for NbS to transform risk management strategies, but it also underscores the urgency of addressing barriers to their implementation. By doing so, we can move towards more sustainable and adaptive coastal communities, better equipped to face the uncertainties of a changing climate.

2. Management and restoration of salt marshes and seagrass meadows in the Venice Lagoon

The Venice Lagoon, one of the largest and most critical transitional ecosystems in the Mediterranean (Tagliapietra et al., 2009), is a shallow back-barrier lagoon located in the northwestern Adriatic Sea, Italy. It spans approximately 550 km², has a mean depth of 1.5 m, and is characterized by a semi-diurnal, micro-tidal regime with an average tidal range of 1 m. Over centuries, human activity has significantly altered this ecosystem, transforming it into a "human-oriented" lagoon that still retains key natural attributes. Major hydraulic modifications—such as river diversions in the 15th–16th centuries, canal excavations and construction of jetties at the inlets since the 19th century—have reduced sediment inflows and caused a generalized deepening of the lagoonal beds (Brambati, 2003; D’Alpaos, 2010). Industrial expansion, extensive reclamation of intertidal areas, and subsidence from groundwater extraction (1930–1970) further disrupted the lagoon’s ecological balance. This transformation has led to a significant expansion of subtidal flats at the expense of the intertidal zones. The recent activation of storm-surge barriers to protect Venice from flooding has further modified lagoon hydrodynamics, accelerating the deepening of tidal flats and limiting sediment accumulation on salt marshes (Mel et al., 2021; Tognin et al., 2021). With negligible contributions from external fluvial and marine sediment sources, current sediment deposition is mainly sourced from the resuspension, reworking, and redistribution of internal lagoon sediments by hydrodynamic processes, including tidal currents, wind-driven waves, and storm surges (Tognin et al., 2021). Over the centuries, the extent of salt marshes in the Venice Lagoon has drastically declined, from approximately 180 km² in 1811 to only around 43 km² by 2002 (Carniello et al., 2009; D’Alpaos, 2010; Tommasini et al., 2019). This loss has been particularly pronounced in the central lagoon, whereas the northern sections have retained more of their natural configuration. Additionally, seagrass meadows have suffered significant declines due to eutrophication, macroalgal blooms, and hydraulic and mechanical clam harvesting.

This degradation has severely affected the lagoon’s biodiversity and ecosystem stability, further emphasizing the need for effective restoration and conservation strategies.

Following the catastrophic flooding of 1966, the Italian government enacted the "Special Law for Venice" (Law n. 171, 1973) to protect Venice and its lagoon from future flooding. This legislation declared “the preservation of Venice and its lagoon as a matter of paramount national interest” and introduced the concept of a basin-wide management policy (Quintana et al., 2018). In 1984, general criteria were established to address the hydrogeological stability of the lagoon, with initiatives to “conduct studies, projects, experiments, and works for the hydrogeological balance of the lagoon, to halt and reverse basin degradation.” This framework led to the first restoration efforts in the 1980s (Quintana et al., 2018).

Additionally, after the European Commission initiated an infringement procedure against the Italian government in 2005 concerning the MOSE project’s impact on biodiversity under the Birds Directive (79/409) and Habitat Directive (92/43) (infringement 2003/4762), a comprehensive compensation plan was introduced by the Venice Water Authority from 2007 to 2011. The plan aimed at conserving and restoring the lagoon’s protected sites included targeted initiatives such as reconstructing salt marshes, restoring tidal flats, and transplanting seagrasses to promote habitat recovery (Quintana et al., 2018). Subsequent restoration projects saw collaborations between universities, research institutes, cooperatives, and local companies, working alongside Venetian authorities. These efforts, often funded by the EU LIFE programme, have expanded on early restoration initiatives with targeted, evidence-based projects (Quintana et al., 2018).

The initial attempts to safeguard the salt marshes in Venice relied on traditional approaches that often resulted in significant environmental impacts during construction. These methods struggled to replicate the intricate natural systems developed over centuries and proved challenging to implement on a large scale. A more

effective and environmentally friendly approach to restoration involves the use of NbS, which leverage local natural resources and guide natural processes. This approach ensures minimal environmental and landscape impact, cost-effectiveness, and delivers social benefits to the local communities involved. Many projects in the Venice Lagoon have embraced NbS, including Life Natura, Life Vimine (<https://www.lifevimine.eu>), Life Lagoon Refresh (<http://www.lifelagoonrefresh.eu>), and Life Seresto (<http://www.lifesteresto.eu>).

2.1. Large-scale restoration under the Venice Special law

The restoration projects inspired by the Venice Special law, managed by Consorzio Venezia Nuova (CVN), have encompassed canal excavations, reconstruction of intertidal flats and salt marshes, renaturalization of previously reclaimed industrial areas, and interventions on subtidal areas to reduce wave shear stress and enhance the stability of the lagoonal beds through seagrass transplantation. This initiative led to the restoration or creation of 106 salt marshes, covering approximately 11 km². Additionally, 18 tidal flats spanning 2 km² were constructed (Volpe, 2012).

Salt marsh restoration included rebuilding eroded areas, protecting vulnerable edges, raising low marshes, and constructing new salt marshes (Nascimbeni, 2007). The restoration process primarily involved creating containment barriers along designated perimeters, where fluidized muddy sediment was pumped in to reach the target elevation. Suitable sediments for salt marsh restoration were sourced from lagoon canal excavations, necessary to restore water flow and navigation channels (Volpe, 2012).

2.2. Life Natura salt marsh protection and restoration through natural engineering techniques at Palude dei Laghi

The LIFE project NATURA “*Barene: Protection and Restoration through Natural Engineering Techniques*”, led by the Venice Water Authority in collaboration with the Coastal Research Center of the Lower Saxony Ministry of Environment, the Technical University of Berlin, and the City of Venice, addressed the issue of salt marsh loss and the degradation of associated habitats of community interest. The project’s main objective was to restore and protect sections of salt marshes, tidal flats, and seabeds in the northern lagoon area near Burano, particularly in the “Palude dei Laghi.” Conducted from late 1999 to early 2002, the project tested various natural engineering interventions to enhance sediment deposition without disturbing the ecological, morphological, hydrodynamic, and landscape characteristics of the marshes. The interventions were tailored to the local conditions of each area, such as wave exposure, depth, and erosion levels. Techniques tested included:

- Placement of “buzzoni” and “burghe” barriers¹ along marsh edges in areas with low and high erosion, respectively, to protect against erosion and help contain sediment.

¹ **Burga:** A conical framework filled with earth, gravel, stones, or similar materials, used to protect riverbanks from erosion caused by water. The framework is constructed with poles or flexible rods, with a base diameter of 1–1.5 meters and a height of 4–5 meters. Due to their shape, burghe are not well-suited for regular defense but are sometimes replaced with buzzoni (see below).

Buzzone: A cylindrical structure used for riverbank protection, similar in materials to burghe but differing in shape and construction. Buzzoni are typically less than 3 meters long with a diameter of about 1 meter. They are reinforced with metal wire bindings, and some may use galvanized iron frameworks for added durability.

- Fascine² barriers behind the marshes, near tidal flats, to reduce wave action and create calm waters that support pioneer halophyte growth and sedimentation.
- Installation of anti-erosion structures along lagoon beds adjacent to marsh edges, consisting of a floating net that promotes the encroachment and growth of bivalves and algae. This structure, made from biodegradable materials (jute sacks treated with linseed oil and cork elements), slows currents to enhance sedimentation.
- Morphological reconstruction through replenishment along consolidated margins and within the marsh edges defined by fascines.
- Substrate stabilization by planting pioneer halophytes, grown in a specially established nursery, to consolidate the soil. The project identified the most successful species for cultivation and replanting, including *Puccinellia palustris* and *Spartina maritima*.

Additionally, as part of the project's awareness campaign, the City of Venice introduced regulations to limit boat speeds, targeted at reducing wave-induced erosion of marsh edges – which is the primary source of wetland loss within the Lagoon.

The most effective techniques from this project are now used throughout the lagoon to restore further marsh areas, replacing rigid embankments with more natural, flexible solutions.

2.3. Life Vimine salt marsh soil-bioengineering

The LIFE VIMINE project (2013–2017) was a demonstrative initiative in the northern Venice Lagoon, developed to establish and test an "integrated approach" for protecting interior, remote salt marshes that are challenging to access. This approach focused on preventing erosion through small-scale, spatially-diffuse soil-bioengineering protection measures, which were designed to minimize environmental and visual impacts. Key to this project were brushwood fascines, each around 2 meters long and 35–40 cm in diameter, sometimes wrapped in coconut netting and bound with biodegradable materials like sisal cords or iron wire. These fascines were strategically positioned based on the local morphology and its observed evolution to address erosion in a way that aligned with natural processes.

Using biodegradable, natural materials, the approach leveraged nature-based solutions: for instance, marsh plants were encouraged to strengthen and enrich the soil with carbon, trap suspended sediments, and gradually build up the marsh platform. This eco-friendly method highlighted how the natural functions of plants could complement and strengthen bioengineering solutions. Additionally, assembling and maintaining these protection structures relied on semi-manual labor, involving local workers to support sustainable local development alongside conservation efforts.

The project's cost-benefit assessment underscored that the expenditure on erosion prevention through soil-bioengineering was balanced by the economic benefits of local job creation and the preservation of essential ecosystem services provided by the salt marshes. This assessment serves as a valuable decision-support tool for public authorities considering future investments in sustainable salt marsh maintenance (Barausse et al., 2015).

² Fascine barriers are wooden branches wrapped in a vegetal net and tied together with vegetal cords installed by anchoring them to wooden poles (Barausse et al., 2015). They are used in riverbank protection, slope stabilization, and erosion control.



Figure 1. Examples of fascines produced locally (upper left) and then placed to protect salt marsh edges from erosion in LIFE VIMINE (Barausse et al., 2015)

2.4. Life Lagoon Refresh: restoration of a brackish marsh environment

The Life Lagoon Refresh project, launched in September 2017, is an active ecological restoration initiative employing an in situ eco-engineering approach to restore the ecotonal environment typical of microtidal lagoons in the northern Venice Lagoon. This environment is characterized by a pronounced salt gradient and extensive intertidal zones vegetated with reedbeds (primarily *Phragmites australis*), which have been significantly reduced due to decades of human intervention. The recreation of the characteristic salt gradient was achieved through the diversion of a freshwater flow from the Sile River into the lagoon and the creation of an intertidal morphology designed to slow freshwater dispersion. The project's actions included the planting of *Phragmites australis* to accelerate reedbed development, the transplantation of small clumps of seagrass species to promote the recolonization of low-salinity aquatic environments by aquatic plants, and the establishment of a 70-hectare protected zone to regulate hunting and fishing pressures.

The project's outcomes were set to be evaluated over a five-year period following its conclusion, with monitoring activities still ongoing. One key result, the restoration of the salinity gradient, has already been achieved as planned in the 70-hectare intervention area. Before the project, the entire area had an annual mean salinity of >30. Post-intervention measurements revealed salinity levels of less than 5 in 5 hectares, less than 15 in 25 hectares, and less than 25 across all 70 hectares (Feola et al., 2022). Early assessments of fish fauna have also shown promising results. Preliminary data indicate a notable increase in *P. canestrinii* populations, from 0.1 individuals/100m² to 20 individuals/100m². Additionally, juvenile commercial species, particularly mullets (*Chelon* spp.), have increased near the freshwater inflow. Post-intervention monitoring of halophytes and reedbeds will continue for several years through a combination of field surveys and drone-based assessments. The project aims to create approximately 20 hectares of reedbeds, with monitoring activities still ongoing to evaluate long-term outcomes.

2.5. Seagrass transplantation initiatives

In recent years, several seagrass transplantation initiatives have been conducted in the Venice Lagoon for environmental restoration. Early experiments (1992–1997) led by the City of Venice involved small-scale transplants in central and southern lagoon areas to determine suitable conditions for native species (*Zostera marina*, *Z. noltei*, *Cymodocea nodosa*) (Quintana et al., 2018). These studies established effective transplanting techniques, including rhizome and sod transplants.

Further restoration by the Venice Water Authority included mechanized transplant methods to enhance resilience, which proved effective in increasing the survival and spread of transplanted seagrass. In 1994, the

Venice Architecture School and Consorzio Thetis conducted larger transplants in the northern lagoon, although the project ultimately failed due to harsh conditions (Quintana et al., 2018).

Between 1996 and 1997, additional trials tested the viability of sod and rhizome transplants at multiple sites, showing success after two growing seasons, with significant gains in *C. nodosa* biomass from sod methods (Quintana et al., 2018).

In 2010, a large-scale mechanized transplantation aimed to restore Sites of Community Importance (SCI) and Special Protection Areas (SPA) in the lagoon. This effort saw 2,250 m² of *C. nodosa* transplanted, leading to substantial coverage increases and low mortality rates, with donor sites fully recovering within three years (Quintana et al., 2018).

In 2012, the EU-funded SeResto project aimed to restore habitat 1150* in the northern lagoon by encouraging widespread transplantation to speed up recolonization. Fishermen planted around 42,670 rhizomes across 35 sites, achieving 0.16–0.22 cm daily growth rates, with natural tidal and wind-driven dispersion aiding recolonization. By year three, 33 of 35 sites had successful colonization (>60%) along salt marsh and canal edges, significantly improving the ecological status from “Poor” to “Good” as measured by Macrophyte Quality Index (MaQI) and Habitat Fish Bioindicator Index (HFBI) indices (Sfriso et al., 2021; Scapin et al., 2016.).

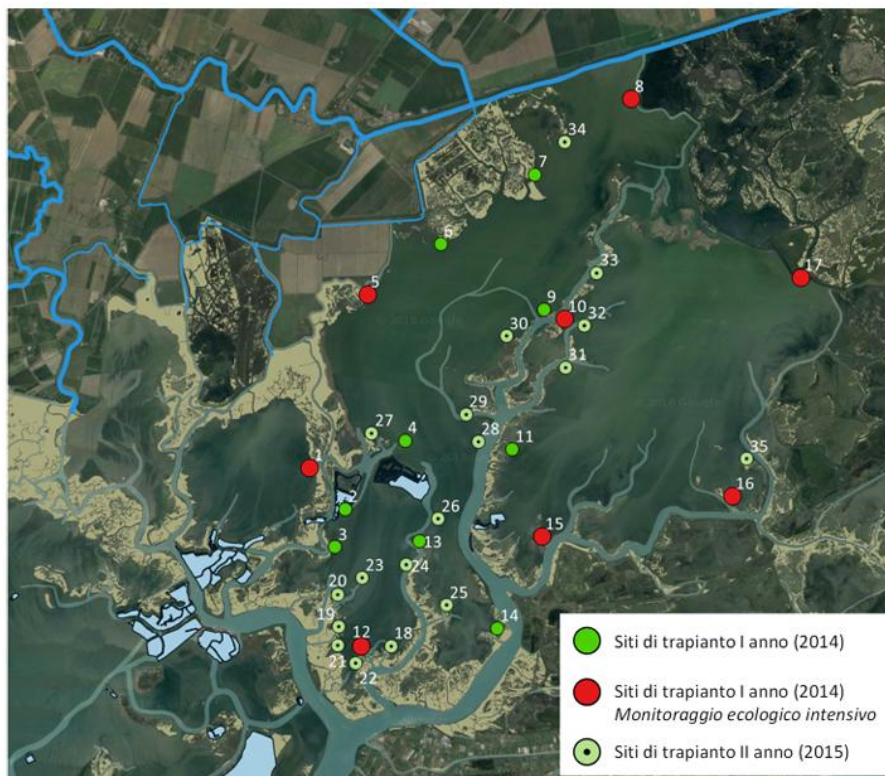


Figure 2. Seagrass transplantation sites in the LIFE SeResto project (green) and monitoring sites (red) (Bonometto et al., 2018).

3. Exploring morphodynamic co-benefits of salt-marsh restoration: insights from the Venice Lagoon (Italy)

3.1. Introduction

Salt marshes are typically located in the upper intertidal zone, and are ecologically and economically significant. They contribute substantially to coastal primary production, support high biodiversity, and provide valuable ecosystem services (Barbier et al., 2011; Costanza et al., 1997; Mitsch & Gossilink, 2000).

Until the mid-20th century, salt marshes were undervalued and often regarded as wastelands awaiting reclamation for agriculture, urban expansion, or waste disposal. However, in recent decades, their extraordinary biodiversity and the critical ecological functions they perform have been increasingly recognized.

Below is a brief overview of some of the key ecosystem services provided by salt marshes, showcasing their indispensable role in supporting both natural systems and human communities:

- Coastal protection and wave attenuation: salt marshes act as natural buffers, where waves break in shallow coastal waters and dissipate energy, reducing erosion and sediment transport. Healthy salt marsh complexes, with wide intertidal flats, divert wave-breaking and erosion away from critical flood defenses and vulnerable areas.
- Surge attenuation: extensive salt marsh areas can mitigate the impact of storm surges by increasing friction as surges propagate into estuaries, similar to wave attenuation but on a larger scale.
- Sediment trapping: functioning salt marshes have a natural ability to trap and retain sediment, maintaining an equilibrium elevation relative to the tidal frame. This resilience to erosion allows for natural recovery following erosive events such as storms.
- Carbon cycling and storage: salt marshes are vital blue carbon ecosystems, storing carbon outside of the tropics. They bury carbon at a higher rate and store more carbon per unit area below ground than their subtidal (e.g., seagrass) and terrestrial (e.g., forests) counterparts. This contributes to climate regulation by sequestering carbon dioxide (CO₂) through carbon burial and long-term storage, owing to the highly productive ecosystem, depositional environments, and low oxygen concentrations in the sediments.
- Water purification: salt marshes in sheltered water bodies, like estuaries and coastal embayments, play a crucial role in regulating water quality. They can reduce concentrations of fecal organisms and absorb heavy metals from the water, thus improving water quality.
- Ecological service provisioning: salt marshes are highly productive ecosystems, supporting diverse communities of salt-tolerant species. They provide essential resources and habitat structures for bird breeding, wintering, and migratory activities, as well as serving as important fish nursery grounds. Abundant marine invertebrates found in these habitats serve as a food source for various species, including birds, fish, and terrestrial animals like voles and small mammals. Additionally, intertidal marshes are vital nursery and feeding areas for young fish and commercially important shellfish.
- Cultural and touristic value: coastal salt marshes contribute to the natural landscape and cultural heritage. Some are even designated as UNESCO World Heritage sites, like "Venice and its lagoon," making them attractive tourist destinations (Hudson et al., 2021).

Hence, coastal salt marshes are of paramount ecological, geomorphological, and socio-economic importance. However, the sustainability of salt-marsh ecosystems is severely threatened by climate changes and increasing anthropogenic pressures. (A. D'Alpaos, 2011; A. D'Alpaos & Marani, 2016; Fitzgerald & Hughes, 2019;

Mudd, 2011; Ratliff et al., 2015; Silvestri, 2018). As a result, extensive salt-marsh areas are being lost worldwide every year at alarmingly increasing rates (Carniello et al., 2009; Day et al., 2000; DeLaune & Pezeshki, 2003; Gedan et al., 2009; Tommasini et al., 2019).

To counteract marsh loss and restore the related ecosystem services, several conservation and restoration projects have been and are still being implemented worldwide. While these efforts are undoubtedly commendable and intrinsically valuable for restoring vital landscape features and supporting biotic interactions, there is a notable lack of studies demonstrating the co-benefits of marsh restoration in terms of morphodynamics—namely, the positive effects on hydrodynamics and sediment transport processes, such as reducing peak tidal levels and enhancing sediment retention.

To address this knowledge gap, here we aim to explore how marsh restoration can influence the morphodynamics of low-lying, shallow coastal areas, with a specific focus on the impact of extensive restoration projects on hydrodynamic and sediment transport processes. The overarching goal of this chapter is to determine whether marsh restoration alone is sufficient to restore coastal systems that have suffered significant degradation due to the complex interplay of natural processes and human activities, ultimately returning them to a more natural, pristine state. Hence, we will explore the co-benefit of marsh restoration for coastal morphodynamics, taken here as the effects of marsh restoration on hydrodynamics and sediment transport processes.

3.2. Materials and Methods

The analyses focus on the microtidal lagoon of Venice, where interactions between natural processes and human activities have driven significant morphological changes over the past 150 years (Luigi D'Alpaos, 2010; Finotello et al., 2023). Established numerical methods are employed to model the morphodynamics of shallow coastal landscapes influenced by tides and waves (Defina, 2000; Carniello et al., 2005, 2011, 2012; D'Alpaos et al., 2007). The study begins by examining changes in lagoon morphodynamics from 1901 to the present, followed by an assessment of the potential impacts of extensive marsh restoration projects designed to restore marsh areas to their historical extents, as identified in historical maps.

The significance of this research extends beyond the Venice lagoon. The methodologies applied and the resulting insights are transferable to other shallow coastal systems with morphodynamic characteristics similar to those of the Venice lagoon. Such environments are widespread globally, including along the East and Gulf coasts of the United States, Northern Europe, Australia's eastern coastline, and the Atlantic coasts of South America. Hence, this study provides a basis for further systematic exploration of the co-benefits of marsh restoration projects on morphodynamics in shallow tidal embayments.

3.2.1. Geomorphological setting

Situated in the northern Adriatic Sea, the Venice Lagoon covers an area of 550 km², making it the largest brackish waterbody in the Mediterranean Basin. This lagoon took shape over a span of 7500 years, formed by the gradual deposition of Late Pleistocene alluvial sediments, locally referred to as Caranto (Zecchin et al., 2008). The contemporary configuration of the lagoon features three main inlets, proceeding from North to South: Lido, Malamocco, and Chioggia (Figure 3a,b,c,d).

Tidal patterns within the lagoon adhere to a semidiurnal microtidal regime, with an average spring tidal range of 1 meter and maximum tidal fluctuations of approximately 0.75 meters relative to Mean Sea Level (MSL) (A. D'Alpaos et al., 2013; Valle-Levinson et al., 2021). Meteorological phenomena often coincide with astronomical tides, resulting in notably high or low tides when atmospheric pressure is low or high,

respectively. Furthermore, wind-related processes play a pivotal role in influencing the hydrodynamics and morphodynamics of the lagoon. Seasonal wind-storm events have a pronounced impact on morphodynamic changes over timescales ranging from decades to centuries (Carniello et al., 2009, 2012). Detailed assessments of the wind climate reveal minimal year-to-year fluctuations in wind energy. The wind-storm events that have the most significant morphological and hydrodynamic effects are those associated with Bora and Sirocco winds (Figure 3e). The north-easterly Bora winds, which blow nearly parallel to the lagoon's major axis, create substantial water-level changes in the southern region of the lagoon and generate large waves with significant wave heights exceeding 1 meter. These waves have a considerable impact on resuspending sediments from the tidal mudflats. Conversely, the south-easterly Sirocco winds induce substantial water-level changes in the northern Adriatic Sea and are often responsible for extensive flooding in Venice and other communities within the lagoon.

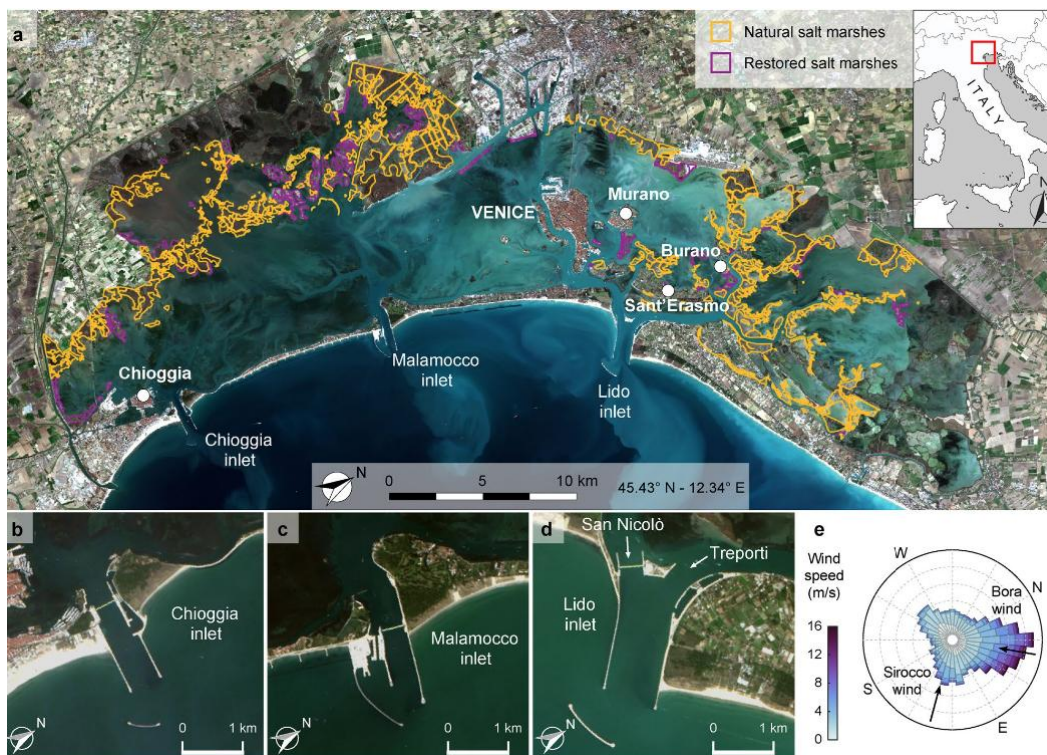


Figure 3: Geomorphological Setting. (a) The Venice Lagoon captured in satellite imagery (Copernicus Sentinel, 2020). Natural salt marshes are outlined in yellow, while restored salt marshes are depicted in purple. (b, c, d) Detailed views of the three primary lagoon inlets. (e) A rose-diagram illustrating the wind climate data recorded at the "Chioggia Diga Sud" anemometric station from 2000 to 2019. Notably, it highlights the two predominant winds: the north-easterly Bora wind and the south-easterly Sirocco wind. (Image © Finotello et al., 2023).

Simultaneously, the extraction of groundwater and natural gas for industrial purposes hastened the natural subsidence of the soil (Carbognin et al., 2004; Gatto & Carbognin, 1981; Zanchettin et al., 2021).

To facilitate the passage of increasingly larger vessels within the lagoon, two major waterways, the Vittorio Emanuele and the Malamocco-Marghera channels (Figure 4), were excavated in 1925 and 1968, respectively. Significant transformations in the lagoon's hydrodynamics arose from the construction of jetties at the lagoon inlets, designed to ensure adequate water depths for commercial ship traffic. The construction of these jetties, spanning different time periods at various inlets, resulted in several changes.

The construction of these jetties significantly narrowed the inlets, as anticipated during the design phase, deepening the water in the process. However, these structures brought about critical alterations in the

hydrodynamic and morphodynamic regimes of the lagoon. The construction of the jetties caused more sustained changes in the lagoon's tidal regime than the typical periodic variations, which are a consequence of the nodal modulation of tides in the Adriatic Sea, typically accounting for about 4% of the characteristic tidal range (Amos et al., 2010; Valle-Levinson et al., 2021). Between 1909 and 1973, the average tidal range within the lagoon surged by up to 25% (Luigi D'Alpaos, 2010; Ferrarin et al., 2015; Tomasin, 1974), with local changes potentially being even more significant (Finotello et al., 2019, 2022; Silvestri, 2018).

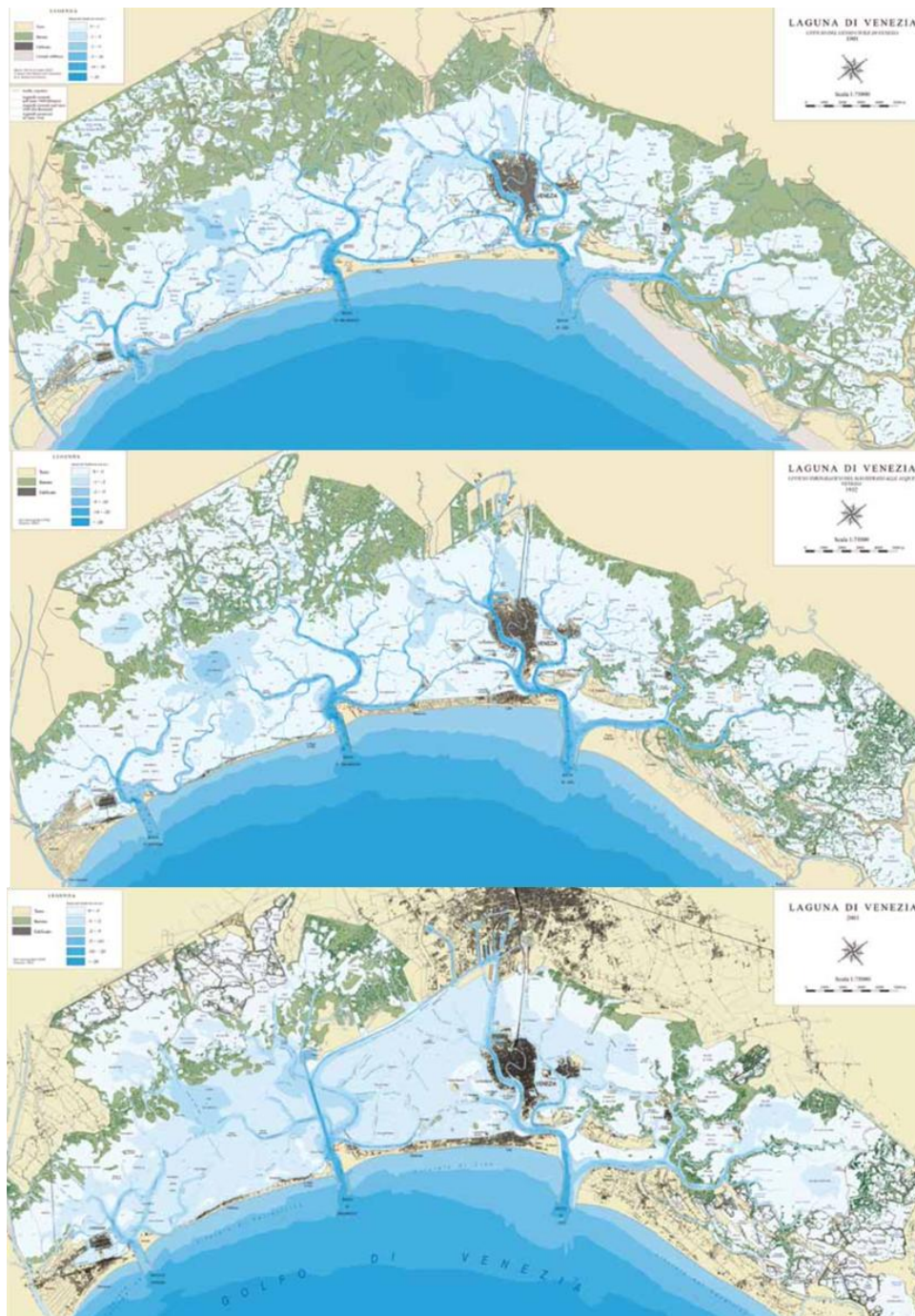


Figure 4: Morphological evolution of the Venice lagoon based on available historical bathymetric maps; (from top) 1901, 1932, 2003. (L. D'Alpaos, 2010)

The alterations in the lagoon's hydrodynamics due to the construction of jetties, in combination with the rise in eustatic sea level (with an average rate of 1.23 ± 0.13 mm/year between 1872 and 2019; and 2.76 ± 1.75 mm/year between 1993 and 2019; Zanchettin et al., 2021), had a significant impact on the lagoon's morphological evolution. This led to the initiation of positive morphodynamic feedbacks, causing larger sections of the lagoon to become ebb-dominated, particularly in the vicinity of the inlets where the jetties introduced strong flow imbalances. These imbalances in tidal flows facilitated the outward transport of fine sediments and impeded the import of sediment carried in suspension by longshore currents (Luigi D'Alpaos, 2010).

This situation was aggravated by the anthropogenic-induced reduction of fluvial sediments, leading to a negative sediment budget and the widespread loss of salt marshes (Carniello et al., 2009; Luigi D'Alpaos, 2010; Tommasini et al., 2019). The diminishing marsh coverage resulted in extended wind fetches, promoting the generation of higher, more energetic waves that exacerbated lateral marsh retreat and caused the erosion of tidal mudflats (Carniello et al., 2009; Finotello et al., 2020; Leonardi et al., 2016; Marani et al., 2011; Mariotti & Fagherazzi, 2013; Tommasini et al., 2019). The deepening of the mudflats (Figure 4), amplified by rising eustatic sea levels and both natural and anthropogenic-induced subsidence, led to the generation of even more substantial wind waves, intensifying the erosion of salt marshes and mudflats through a positive feedback loop.

Further human-made modifications were introduced to the inlet morphologies between 2006 and 2014 to accommodate the mobile floodgates of the Mo.S.E. (short for "Modulo Sperimentale Elettromeccanico," or Electromechanical Experimental Module) system. This system was designed to protect the city of Venice and other lagoon settlements from extensive flooding (Mel et al., 2021). These interventions marginally increased hydraulic resistances at the inlets, resulting in a reduction of tidal amplitudes and an increase in tidal-phase delays within the lagoon (Ghezzi et al., 2010; Matticchio et al., 2017).

3.2.2. Salt marshes in the Venice lagoon: current state

Salt marsh erosion persists today, albeit at a significantly reduced areal extent compared to the previous century. This is attributable to a series of critical interventions aimed at safeguarding and restoring salt marshes, initiated by the Venice Water Authority since the early 1990s, with additional contributions from some EU-funded LIFE projects (Barausse et al., 2015; Tagliapietra et al., 2018; Tommasini et al., 2019), as described in Chapter 2.

Currently, approximately 12% of existing salt marshes have been either entirely artificially created or partially restored (Figure 3), with a substantial portion of the remaining natural marshes being protected against lateral erosion through the use of manmade wooden piles or bundles of sticks. It is evident that without these restoration and conservation efforts, the total area of salt marshes would be significantly smaller than it is today.

Lastly, it's worth noting that the operation of the Mo.S.E. floodgates will further diminish the resilience of salt marshes against rising relative sea levels, primarily by reducing inorganic deposition during storm-surge events, which, although sporadic, play a crucial role in marsh vertical accretion (Tognin, 2022; Tognin et al., 2021).



Figure 5: Google Earth photo showing artificial salt marshes in the southern Venice lagoon near Chioggia.



Figure 6: Marsh restoration using nature-based solution (<https://www.lifevimine.eu>).

3.2.3. Numerical modeling

To investigate the impacts of marsh restoration on morphodynamics, a two-dimensional, depth-averaged, finite-element numerical model was employed. The model consists of three interconnected modules: the hydrodynamic module coupled with the wind-wave module (WWTM) (Carniello et al., 2011) and the sediment transport and bed evolution module (STABEM) (Carniello et al., 2012). This model is well-suited for simulating sediment dynamics that govern the morphodynamic evolution of shallow micro-tidal basins.

The hydrodynamic module solves the two-dimensional depth-integrated shallow water equations (SWEs), which are phase-averaged over a representative elementary area characterized by irregular topography to account for very shallow flows, wetting, and drying (Defina, 2000). In a Cartesian frame (x, y) , these SWEs can be expressed as follows:

$$\vartheta(\eta) \frac{\partial \eta}{\partial t} + \nabla \cdot \mathbf{q} = 0 \quad (1)$$

$$\frac{D}{Dt} \left(\frac{\mathbf{q}}{Y} \right) + \frac{1}{Y} \nabla \cdot \mathbf{Re} + \frac{\boldsymbol{\tau}_t}{Y\rho} - \frac{\boldsymbol{\tau}_s}{Y\rho} + g\nabla h = 0 \quad (2)$$

In the equations, several symbols and terms are defined as follows:

- t represents time.
- η is the free surface elevation measured relative to a datum.
- $q = (q_x, q_y)$ represents the depth-integrated velocity, indicating discharge per unit width.
- ∇ and $\nabla \cdot$ denote the 2D gradient and divergence operators, respectively.
- The symbol ϑ represents the wet fraction of the computational domain, which depends on water depth and local topographic irregularities (Defina, 2000).

In the momentum equation (Eq. 2), D / Dt represents the material (or Lagrangian) time derivative, while Y represents the water volume per unit area, equivalent to the water depth. τ_t and τ_s are the shear stresses at the bottom (due to tidal currents) and at the free surface (due to wind drag), respectively. Additionally, ρ denotes water density, and g represents gravity.

The Reynolds stresses are computed using a depth-averaged version of Smagorinsky's model (Smagorinsky, 1963) and can be expressed in tensor index notation as follows:

$$\mathbf{Re} = R_{ij} = \nu_e Y (u_{i,j} + u_{j,i}) \quad (3)$$

$$\nu_e = 2C_S^2 A_e \sqrt{2(u_{x,x})^2 + (u_{x,y} + u_{y,x})^2 + 2(u_{y,y})^2} \quad (4)$$

In equation (3), the indices i and j represent either the x or y coordinates, while $u = q/Y$. The eddy viscosity, denoted as ν_e , is proportional to the strain rate and involves parameters such as A_e , which represents the area of the computational element, and C_S , which is the Smagorinsky coefficient with a value of 0.2.

The numerical scheme employs a mixed Eulerian-Lagrangian approach, where the material derivative in equation (2) is computed as a finite difference in time and solved using the method of characteristics. This approach enables solving the continuity equation (1) with a semi-implicit scheme, resulting in a self-adjoint spatial operator. The solution is achieved on a staggered triangular grid using the finite element method of Galerkin, as described by Defina (2000), and flow rates are obtained through back-substitution.

The wind-wave module, as presented by Carniello et al. (2011), resolves the wave action conservation equation on the same computational grid as the hydrodynamic module. The wind-wave module utilizes water depths and depth-averaged flow velocities from the hydrodynamic module to propagate the wind-wave field. The evolution of the wave action density (N_0) in the frequency domain is governed by the equation presented in Carniello et al. (2011).

$$\frac{\partial N_0}{\partial t} + \frac{\partial}{\partial x} c'_{gx} N_0 + \frac{\partial}{\partial y} c'_{gy} N_0 = S_0 \quad (5)$$

The wind-wave module, as explained by Carniello et al. (2011), calculates the group celerity components, c'_{gx} and c'_{gy} , to approximate the propagation speed of N_0 . The source terms related to wind-wave effects, collectively represented as S_0 , encompass both positive (wind energy input) and negative (bottom friction, whitecapping, and depth-induced breaking) contributions to wave energy. Wave period distribution is determined based on the relationship between peak-wave period, local wind speed, and water depth, following Young and Verhagen (1996) (Young & Verhagen, 1996). Given the nearly vertical and jagged margins of the lagoon, refraction effects are disregarded, and waves are assumed to propagate in the direction of the wind.

The horizontal orbital velocity at the bottom, derived from significant wave height using linear wave theory, contributes to the bottom shear stress, τ_w , induced by the wind-wave field. Nonlinear interactions between τ_w and current-induced bottom shear stress (τ_t) are considered through the empirical formulation developed by Soulsby (1995), which increases the total bottom shear stress, τ_b , beyond the simple sum of τ_t and τ_w .

Incorporating the same computational grid, the STABEM module, detailed by Carniello et al. (2012), addresses the advection-diffusion equation for suspended sediment with a conservative, second-order spatial scheme. Additionally, it tackles Exner's equation, which describes sediment bed evolution and interactions with the suspended sediment.

$$\frac{\partial C_i Y}{\partial t} + \nabla \cdot (\mathbf{q} C_i) - \nabla \cdot (\mathbf{D}_h \nabla C_i) = E_i - D_i \quad i = s, m \quad (6)$$

$$(1 - n) \frac{\partial z_b}{\partial t} = \sum_i (D_i - E_i) \quad (7)$$

In the equations, C represents the depth-averaged sediment concentration, and $D_h(x, y, t)$ is a two-dimensional diffusivity tensor that varies in space and time. This diffusivity tensor is assumed to be equal to the eddy viscosity computed by the hydrodynamic module, as explained by Viero and Defina (2016) (Viero & Defina, 2016). The terms E and D are associated with the entrainment and deposition of bed sediment, while z_b denotes the bed elevation, and n is the bed porosity, which is assumed to have a constant value of 0.4.

The subscript "i" is used to distinguish between non-cohesive (sand, denoted as "s") and cohesive (mud, denoted as "m") sediment classes that are typically found in the bed of tidal lagoons. The relative content of mud (p_m), representing the sum of clay and silt, is assumed to vary both in time and space. This variation determines whether the sediment behaves in a cohesive or non-cohesive manner and sets the critical value of the bottom shear stress.

A threshold value of mud content ($p_{mc} = 10\%$) is used to distinguish between non-cohesive and cohesive behavior, following Van Ledden et al. (2004). The median diameters D_{50} adopted in the simulations to describe cohesive and non-cohesive sediments are 20 μm and 200 μm , respectively, based on measurements conducted in the Venice Lagoon, as described by Carniello et al. (2012).

The deposition rate of sand D_s is computed as

$$D_s = w_s r_0 C_s \quad (8)$$

Where w_s represents the absolute value of the sand settling velocity, and r_0 is the ratio of near-bed to depth-averaged concentration. In this context, r_0 is considered constant and is assumed to be equal to 1.4, as reported in Parker et al. (1987).

The deposition rate of pure cohesive mud, D_m , is determined by Krone's formula, which can be expressed as:

$$D_m = w_m C_m \max \{0; 1 - \tau_b / \tau_d\} \quad (9)$$

where:

- w_m represents the absolute value of the mud settling velocity.
- τ_b is the bottom shear stress, computed by the hydrodynamic module.
- τ_d is the critical shear stress for deposition, and it is set to a value of 1.0 Pa.

The settling velocities, w_s and w_m , are calculated using the Van Rijn formulation (van Rijn, 1984) for solitary particles in clear and still water. This formulation does not incorporate flocculation effects, which are considered negligible for particle diameters larger than 20 μm (Mehta et al., 1989).

The erosion rate is highly dependent on the degree of cohesion of the sediment mixture. For non-cohesive mixtures (where the mud content p_m is less than the critical value p_{mc}), the erosion rate of sand, E_s is described by the Van Rijn formulation (van Rijn, 1984). Meanwhile, the erosion rate of mud, E_m , can be computed using the formulation proposed by Van Ledden (Van Ledden et al., 2004).

$$\begin{aligned} E_s &= (1 - p_m)w_s \cdot 1.5 \left(\frac{D_{50}/Y}{D_*^{0.3}} \right) T^{1.5} \\ E_m &= \frac{p_m}{1 - p_m} M_{nc} T \end{aligned} \quad \text{for } p_m < p_{mc} \quad (10)$$

For cohesive mixtures ($p_m > p_{mc}$), both sand and mud erosion rates can be computed using the Partheniades's formula

$$\begin{aligned} E_s &= (1 - p_m) \cdot M_c T \\ E_m &= p_m \cdot M_c T \end{aligned} \quad \text{for } p_m > p_{mc} \quad (11)$$

In equations (10) and (11), the various parameters are defined as follows:

- D_* is the dimensionless grain size and is calculated as $D_{50} [(s - 1)g / \nu^2]^{1/3}$, where D_{50} is the median sediment diameter, s is the sediment's specific density, ν is the water's kinematic viscosity, g represents the gravitational acceleration.
- T is the transport parameter.
- M_{nc} and M_c are specific entrainment values for non-cohesive and cohesive mixtures, respectively.

These entrainment values are based on formulations provided by Van Ledden et al. (2004) and van Rijn (1984):

$$M_{nc} = \alpha \frac{\sqrt{(s - 1)gD_{50}}}{D_*^{0.9}}, \quad M_c = \left(\frac{M_{nc}}{M_m} \cdot \frac{1}{1 - p_{mc}} \right)^{\frac{1 - p_m}{1 - p_{mc}}} \cdot M_m \quad (12)$$

where M_m is the specific entrainment for pure mud ($M_m = 5 \cdot 10^{-2} g m/s$) and α is set equal to $1 \cdot 10^{-5}$.

The transport parameter is usually defined as $T = \max\{0; \tau_b/\tau_c - 1\}$, where τ_b represents the local bottom shear stress, and τ_c is the critical shear stress for erosion. This definition results in a sharp transition between $T = 0$ and $T = \tau_b/\tau_c - 1$. However, in real tidal systems, both τ_b and τ_c vary in space. Therefore, it is assumed that they are both random variables and follow a log-normal distribution, as described in Carniello et al. (2012). This stochastic approach leads to a smoother transition between $T = 0$ and $T = \tau_b/\tau_c - 1$.

All the model parameters fall within the range of variability of similar deposition and erosion formulations (Breda et al., 2021; Temmerman et al., 2005). Notably, erosion is set to zero on salt marshes because the presence of vegetation reduces velocity and wave energy, protecting the sediment from erosion (Möller et al., 1999; Temmerman et al., 2005).

The combined effect of erosion and deposition fluxes of sand and mud results in a variation in bed level over time, which is calculated based on equation (8).

The model has been extensively tested and validated against hydrodynamic, wind-wave, turbidity, and satellite data from various locations, including the Venice Lagoon (Italy), Virginia Coast Reserve lagoons (USA), and Cadiz Bay (Spain), as documented in previous studies (Carniello et al., 2011, 2014; Mariotti & Fagherazzi, 2010; Zarzuelo et al., 2018).

3.2.4. Numerical simulations

Numerical simulations were conducted using five distinct morphological configurations of the Venice Lagoon. Three configurations represent historical lagoon morphologies reconstructed from available topographic and bathymetric data (Figure 4), corresponding to the years 1901, 1932, and 2014 (i.e., present day). Each computational grid accurately reflects the lagoon's characteristics based on the respective topobathymetric surveys. The 1901 grid was derived from the "Topographic/Hydrographic Map of the Venice Lagoon" produced by the Genio Civile of Venezia, which includes the jetties at the Lido inlet constructed by that time. The 1932 and 2014 grids were developed using topographic surveys conducted in 1932 and 2003 by the Venice Water Authority (Magistrato alle Acque di Venezia). The 2014 configuration incorporates anthropogenic modifications at the three inlets due to the Mo.S.E. system, completed in that year.

Detailed calibration of the hydrodynamic and wind-wave models, as well as their applications to the Venice Lagoon, are documented in Carniello et al. (2005, 2011) and Tognin et al. (2022). Model calibration and testing were primarily focused on recent lagoon configurations for which field data are available. For older configurations (1901, 1932), local bed-friction coefficients were estimated based on calibrated grid values while accounting for factors such as sediment grain size, bed elevation, and potential vegetation presence, particularly in salt marshes.

The two additional configurations represent hypothetical scenarios characterized by extensive marsh restoration, resulting in significant expansion of marsh areas compared to the present-day morphology. The 2014 computational grid was used as a baseline, with marshes reconstructed based on their spatial distributions observed in 1901 and 1932. Marsh areas were added incrementally, and elements along marsh margins were adjusted to align with their historical positions. Elevation and bed roughness properties were modified to match adjacent tidal flats. These restoration scenarios, referred to as "Restored 1932" and "Restored 1901," allow for analysis of the potential effects of restoring salt marshes to historical conditions. They provide a basis for assessing whether scaling up marsh restoration efforts could have significant impacts on morphodynamic processes, such as hydrodynamics and sediment transport, within the lagoon.

It is worthwhile noting that despite the theoretical influence of marsh creation on the tidal prism (the water volume exchanged between the lagoon and the sea), which could alter inlet cross-sectional areas following the O'Brien-Jarrett-Marchi law (A. D'Alpaos et al., 2009; Jarrett, 1976), inlet geometries remained unchanged in the hypothetical scenarios. This decision reflects the constraints imposed by the fixed horizontal and vertical geometry of the inlets due to jetties and concrete structures associated with the Mo.S.E. floodgates. Additionally, scour processes over the past century have deepened the inlets to the overconsolidated Caranto layer, preventing further significant deepening, even in the absence of the Mo.S.E. barriers.

Concerning boundary conditions for the numerical simulations, water levels were prescribed at the seaward boundary of the computational domain, representing the portion of the northern Adriatic Sea in front of the Venice Lagoon (Figure 7). Water-level data were obtained from measurements taken at the CNR Oceanographic Platform, situated in the Adriatic Sea approximately 15 km from the coastline. As water levels and bed elevations in each computational grid reference mean sea level at the time of each survey, they implicitly account for historical rises in relative sea level. Wind speeds and directions are measured at the "Chioggia Diga Sud" anemometric station and are applied to the entire lagoonal basin (Carniello et al., 2005). Consistent boundary conditions were used for all simulations, enabling direct comparisons between different lagoon configurations. The model was driven by hourly water levels and wind velocities and directions recorded from November 16th, 2005, to December 17th, 2005 (Figure 7). This 30-day period serves as a representative snapshot of the typical hydro-meteorological conditions experienced annually in the Venice Lagoon between October 1st and January 30th, a period known for significant storm-surge events. The cumulative frequency of water levels during this study period closely matches the average distribution

observed between 2000 and 2020 (Figure 7c). Furthermore, the selected study period encompasses two relatively strong Bora wind events, which are characteristic of the wind climate in Venice (Figure 7a). Therefore, this study period allows for a focus on both typical tides and representative storm events.

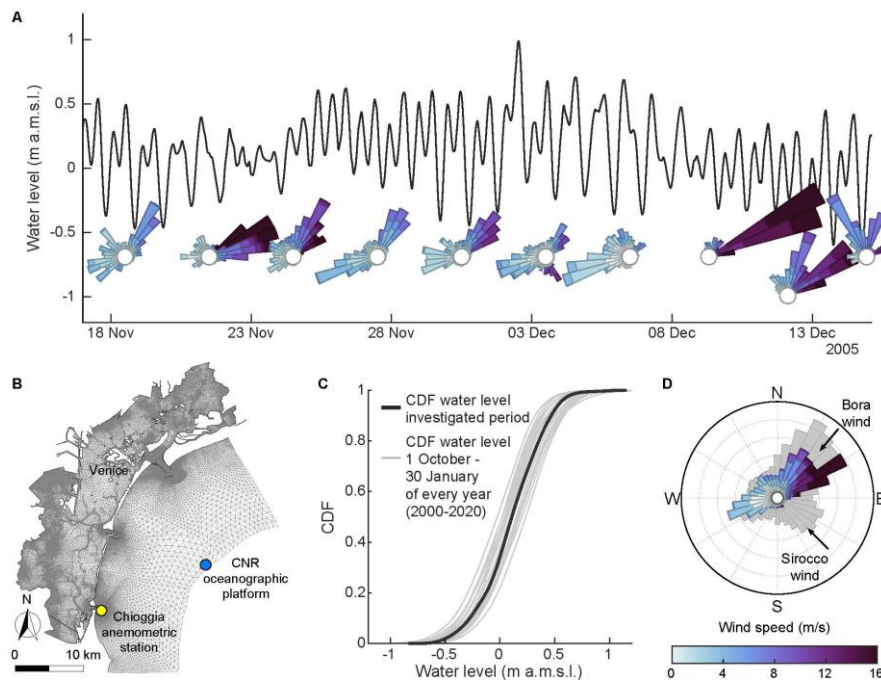


Figure 7: The data used in the numerical simulations pertain to a specific time period from November 17, 2005, to December 17, 2005. Water levels were monitored and recorded at the "CNR Oceanographic Platform," and wind data were collected from the "Chioggia Diga Sud" anemometric station, as depicted in panel (b). The computational grid employed in the numerical model is illustrated in panel (b) and corresponds to the 2014 morphological configuration of the Venice Lagoon. Panels (c) and (d) compare the distributions of water levels (c) and wind climate (d) during the analyzed period to those observed over the period from 2000 to 2019, represented in grey. These comparisons provide valuable context for understanding the conditions simulated in the study. (Image from Finotello et al., 2023)

Notably, a morphological acceleration factor of 12 was employed to accelerate morphological evolution. The use of a morphological acceleration factor is a common practice aimed at reducing the computational time required for extended morphodynamic simulations. This factor is a scalar quantity applied to the Exner's sediment continuity equation, operating under the assumption that morphodynamic changes occur at longer time scales compared to the hydrodynamic processes (e.g., Lesser et al., 2004). The implementation of this morphological acceleration factor allows our month-long simulations to be effectively interpreted as year-long simulations (i.e., one month multiplied by 12) when considering morphological evolution processes, such as salt marsh sedimentation and vertical accretion. It is, however, essential to recognize that, while this approximation is reasonably accurate, the period under analysis is particularly favorable for salt marsh growth. This is due to the significant resuspension of mineral sediment by waves, which is subsequently deposited over salt marshes (Tognin et al., 2021). Consequently, the application of a morphological factor in the way we illustrate may somehow lead to a slight overestimation of annual marsh deposition rates.

3.3. Results and Discussion

3.3.1. Water levels

When comparing maximum water levels modeled for the present-day configuration of Venice Lagoon (i.e., 2014) to past configurations (i.e., 1901 and 1932), a significant variation approximately equal to ± 30 cm on average, became evident, signifying notable hydrodynamic changes (Figure 8a,b). In contrast, the difference between the 2014 conditions and the restored configurations exhibited a smaller range of approximately ± 2.3 cm. This underscores once more that the impact of salt marsh restoration is minimal, with only marginal effects observed in specific locations. These locations are quite distant from Venice's city center and other important inhabited islands of the Lagoon (e.g., Murano, Burano, Torcello, Chioggia, Sant'Erasmus), so there are no discernible benefits in terms of reduction of maximum water levels (Figure 8c,d).

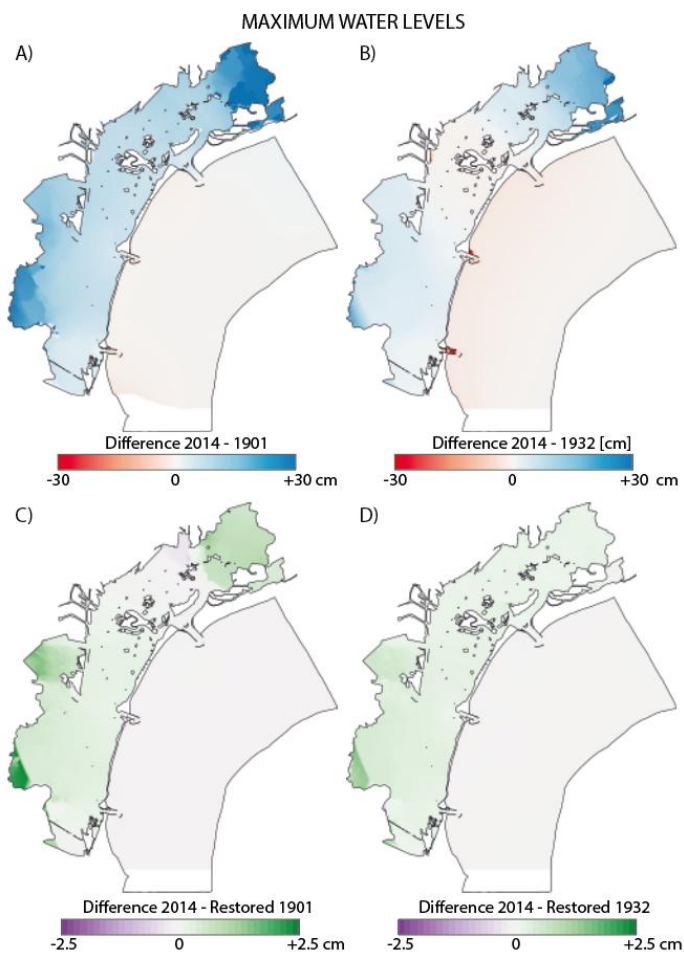


Figure 8: Differences in numerically modeled maximum water levels across the Venice lagoon. Results are presented as maps of differential values between the 2014 (i.e., present-day) configuration of the Venice lagoon and other morphological configurations. A) Differences between 2014 and 1901; B) Differences between 2014 and 1932; C) Differences between 2014 and the “Restored 1901” scenario; D) Differences between the 2014 and “Restored 1932” scenario. Note different colormap scales for panels A-B and C-D.

3.3.2. Significant wind-wave heights

In terms of significant wave heights, the comparison between 2014 and both the 1901 and 1932 configurations exhibit higher spatial variability, with waves being generally higher across extensive tidal flats areas for the

2014 morphological configuration (Figure 9a,b). In contrast, the disparities between 2014 and the restored configuration reveal a distinct trend. A clear pattern emerges over the marsh-restored area, indicating a substantial decrease in significant wave height (i.e., positive value in terms of wave height differential; Figure 9c,d). Marsh restoration thus appears to yield a benefit in this specific area. However, in the majority of the lagoon, denoted by white colors, there are no discernible changes (Figure 9c,d). Similarly, Venice City remains unaffected. This implies that salt marsh restoration alone cannot directly benefit Venice City in terms of reduction of wave height, and related mitigation of sidewalk overtopping and city flooding (Ruol et al., 2020).

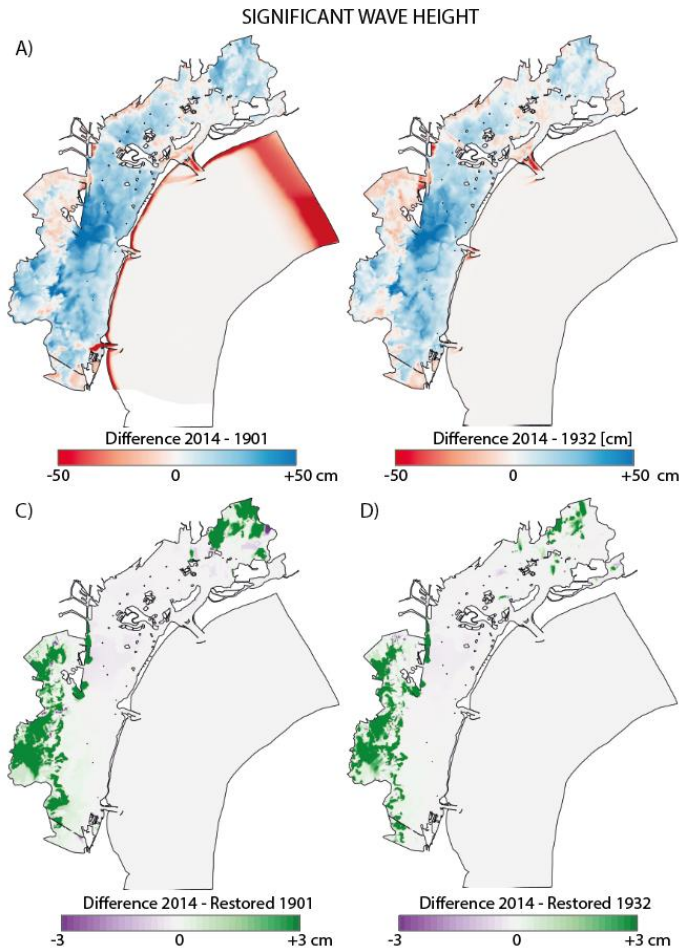


Figure 9: Differences in numerically modeled significant wave heights across the Venice lagoon. Results are presented as maps of differential values between the 2014 (i.e., present-day) configuration of the Venice lagoon and other morphological configurations. A) Differences between 2014 and 1901; B) Differences between 2014 and 1932; C) Differences between 2014 and the “Restored 1901” scenario; D) Differences between the 2014 and “Restored 1932” scenario. Note different colormap scales for panels A-B and C-D.

3.3.3. Bed shear stresses

In concluding the hydrodynamic analysis, a comprehensive spatial-temporal evaluation was performed to assess the combined effects of wind waves and tidal currents, expressed as maximum shear stresses exerted on the lagoon bed. A comparison between present-day and historical configurations (1901 and 1932) indicates higher shear stresses in the current configuration, particularly across extensive tidal flat areas where waves more effectively winnow the bed, especially during intense storm events (Figure 10a,b). Conversely,

reductions in bed shear stress are observed along major tidal channels, likely attributable to the deepening these channels have undergone. Differential maps comparing present-day and restored morphological configurations indicate minimal impacts of marsh restoration, limited to areas where marshes have been reintroduced. This underscores the negligible effect of salt marsh restoration on overall morphodynamic processes (Figure 10c,d).

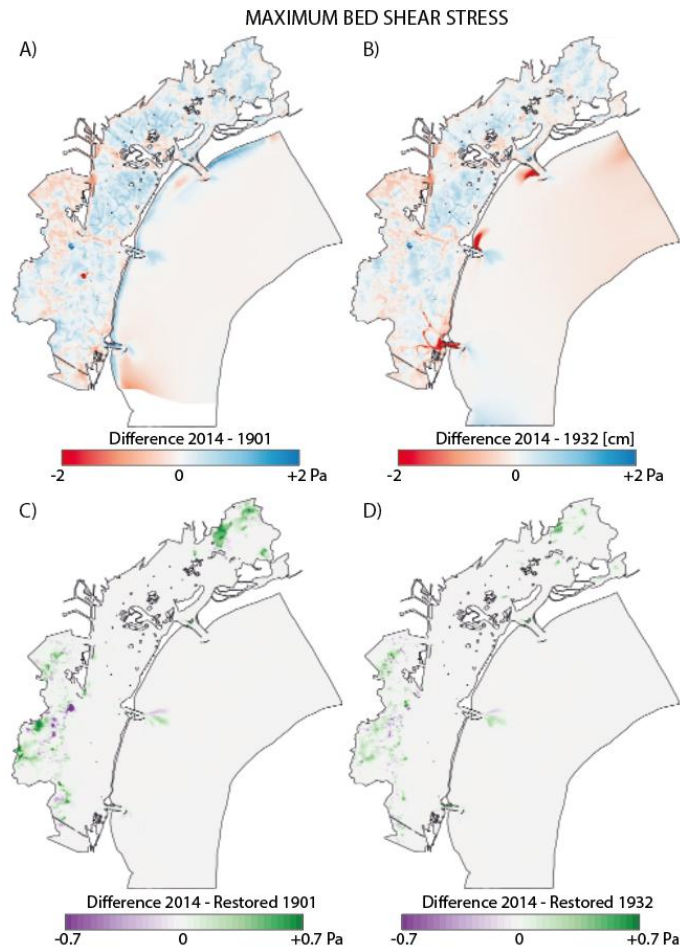


Figure 10: Differences in numerically modeled maximum bed shear stresses across the Venice lagoon. Results are presented as maps of differential values between the 2014 (i.e., present-day) configuration of the Venice lagoon and other morphological configurations. A) Differences between 2014 and 1901; B) Differences between 2014 and 1932; C) Differences between 2014 and the “Restored 1901” scenario; D) Differences between the 2014 and “Restored 1932” scenario. Note different colormap scales for panels A-B and C-D.

3.3.4. Sediment budget at the Lagoon scale

Differences in hydrodynamic forcings drive variations in sediment entrainment, transport, and redistribution across the lagoon, ultimately influencing the morphological evolution of the lagoon bed. The results of the numerical simulations provide valuable insights into the overall sediment budget of the Venice Lagoon, with specific emphasis on salt marsh dynamics.

Figure 11 illustrates the changes in sediment volume distribution across different configurations. A decline in the total sediment volume deposited on salt marshes is observed from 1901 to 1932. Notably, the “Restored” configurations show sediment volumes comparable to those of 2014, indicating a limited impact of restoration on marsh sedimentation dynamics despite an increase in the overall marsh area. Other morphological units

also exhibit significant changes, with tidal flats experiencing decreased sediment deposition, while channels show an increase in deposited sediment volume.

The ratio between the areal extent of salt marshes and the sediment volume deposited on them provides insights into mean vertical accretion rates—a critical factor determining whether salt marshes can keep pace with rising relative sea levels. Figure 12 explores vertical accretion rates across the examined morphological configurations. In the "Restored" configurations, a reduction in mean salt marsh accretion rates is noted compared to the current state (i.e., 2014). This occurs because the total volume of sediment deposited on marshes remains nearly unchanged (Figure 11), while the overall marsh area increases due to restoration efforts implemented in the "Restored" scenarios.

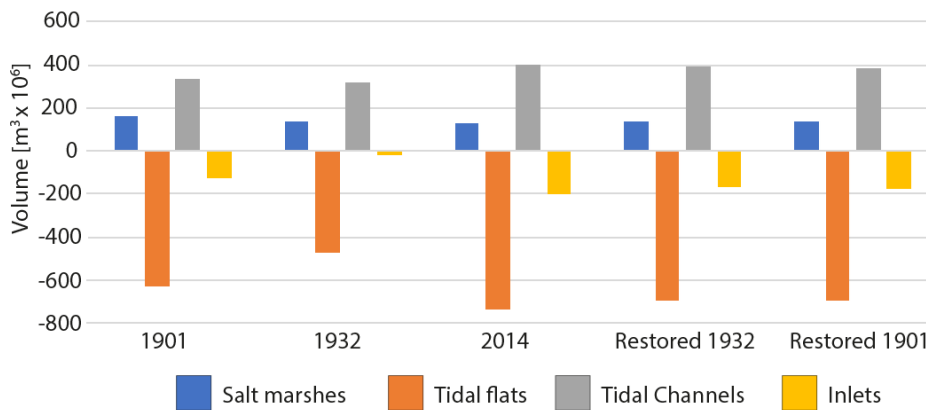


Figure 11: Modeled changes in sediment volumes across different morphological units are presented. For salt marshes, tidal flats, and tidal channels, positive values indicate sediment deposition, while negative values represent erosion. For inlets, sediment volumes are calculated as the integral of sediment flux across all lagoonal inlets, where positive values denote sediment import into the lagoon and negative values represent sediment export to the open sea.

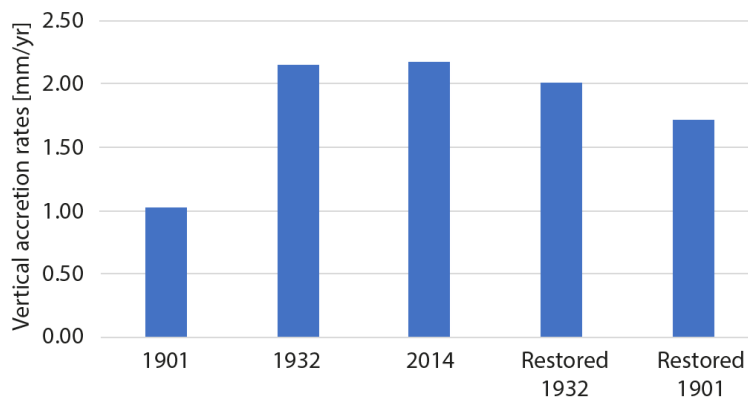


Figure 12: Modelled salt-marsh vertical accretion rates (taken here as the vertical accretion due to mineral sediment deposition alone) for different morphological configurations of the Venice Lagoon.

3.4. Conclusions

Our analyses show that in shallow-water, sediment-starved, and highly anthropogenically modified environments such as the Venice Lagoon, restoring salt marshes in locations where they historically existed before being eroded has negligible effects on the overall estuarine morphodynamics. This is likely because the loss of salt marshes over time typically does not occur in isolation but is accompanied by other morphological changes within the estuarine system. Specifically, in the Venice Lagoon, marsh deterioration has historically coincided with a general deepening of the lagoon bed, resulting in a present-day morphology that is significantly deeper than it was a century ago (see Figure 4). Consequently, the restoration of marshes alone is insufficient to return the system to its historical hydrodynamic state prior to marsh loss. As a result, the impact of marsh restoration on sediment transport processes and the associated morphological evolution of the basin is similarly minimal.

Moreover, and more interestingly, artificially increasing the total marsh area via restoration without altering the total sediment supply to the estuarine system is likely to reduce salt marsh vertical accretion rates. This occurs because the same volume of mineral sediments must be distributed over a larger marsh area. From this perspective, marsh restoration might not only fail to provide significant benefits for estuarine morphodynamics but could also compromise the ability of salt marshes to keep pace with rising relative sea levels through mineral sediment deposition and associated vertical soil accretion.

These findings are not necessarily generalizable to estuarine systems that are morphodynamically different from the Venice Lagoon, particularly those characterized by a net positive sediment budget sustained by fluvial or marine sediment supply, or both. Nevertheless, the methodology employed in this study is easily transferable to other contexts, provided that historical topo-bathymetric data are available to enable accurate morphological reconstruction and, consequently, precise numerical modeling of the estuarine system under investigation.

4. Carbon sequestration potential of salt marsh restoration: insights from the Venice Lagoon Case Study

4.1. Methods

Vegetated coastal ecosystems, including salt marshes, have been termed “Blue Carbon ecosystems” for their increasingly recognized carbon (C) sequestration and storage potential (Chmura et al., 2003; Duarte et al., 2005; Macreadie et al., 2019; McLeod et al., 2011; Nellemann et al., 2009). Estimates show that the C burial rate per unit area in these ecosystems may be exceptionally high, exceeding that of terrestrial forests by 1–2 orders of magnitude (Chmura et al., 2003; Duarte et al., 2005; Macreadie et al., 2019; McLeod et al., 2011). In light of this, tidal wetlands may provide a considerable contribution to global long-term C sequestration, despite their limited areal extension (Chmura et al., 2003; Duarte et al., 2005; Macreadie et al., 2019; McLeod et al., 2011). Additionally, tidal wetlands support many other ecosystem services, whose high value is often difficult to estimate (Barbier et al., 2011). These services include enhancing biodiversity, protecting coastlines from erosion and storm surges, supporting commercial fisheries, filtering nutrients and pollutants, and contributing to tourism and recreational activities (Barbier et al., 2011). Despite this potential, salt marshes are rapidly declining worldwide, prompting significant conservation and restoration efforts to preserve their essential ecological functions and societal benefits. Salt marsh conservation and restoration has emerged as a prominent nature-based solution, offering notable advantages for climate change mitigation and increased coastal resilience. By restoring salt marshes, it is possible to significantly enhance carbon storage capacity. However, uncertainties remain in accurately estimating the carbon sequestration and storage potential of salt marshes, highlighting the need for continued research to optimize their role in global climate mitigation strategies.

To address this, we analysed soil organic content in 10 salt marshes of the Venice Lagoon (Italy) (Puppini et al., 2024). Ten salt marshes were selected in the whole Venice Lagoon, in order to provide a spatially-explicit assessment of C accumulation rates. Six uncompacted cores were collected in each of the 10 selected salt marshes, for a total of 60 cores. The core depth of 1 m was selected as international methodologies for SOC assessment are generally based on analyses over depths of 1 m (Howard et al., 2014). For each core, soil samples were taken at 12 depths (0, 5, 10, 15, 20, 25, 30, 35, 40, 45, 50, 75 cm from the surface, see Howard et al., 2014) and subsamples were prepared for different analyses, including soil density, organic matter and carbon content.

Samples were dried at 60°C until a constant weight was achieved. The difference in weight between wet and dry samples was used to estimate the water content. Percent organic matter of each sample was determined through Loss On Ignition (LOI, at 375°C for 16 hr, Roner et al., 2016). Water content and organic matter content were used to estimate the dry bulk density (DBD) (Kolker et al., 2009). In order to obtain carbon content, we calculated a conversion equation from organic matter (from LOI) into organic carbon using Elemental Analysis on a subset of samples (n=102), following Craft et al. (1991). The Organic Carbon content and soil density measurements enabled the computation of Soil Carbon Density (SCD), as:

$$SCD = OC_i \times DBD_i$$

where OC_i is the organic carbon content and DBD_i is dry bulk density of the i th soil interval.

Carbon accumulation rates were estimated by multiplying the average SCD in a reference surface layer of 5 cm (average value for each location) by salt marsh accretion rates derived from measurements based on marker horizons (over a 2–20 years period) (Puppini et al., 2024). The short-term estimate was chosen due to the

availability of marker horizon data and because it was deemed more reasonable for future projections and comparisons, as it excludes the influence of past extensive modifications of the lagoon. However, using the OC content of a superficial reference layer may lead to an overestimation of the carbon accumulation by neglecting the effect of decomposition on longer timescales. Therefore, in order to provide a comparison, beside the short-term estimate, a long-term estimate is provided on the basis of the average SCD in the top-1-m reference interval and accretion rates determined from ^{210}Pb profiles by Bellucci et al. (2007) (to the depth of 50–60 cm, back to about 100 years ago) (Puppini et al., 2024).

4.2. Results

Estimates of carbon accumulation rates (short-term) were used to assess CO_2 sequestration by salt marsh soils in the Venice Lagoon, converting the mass of carbon into CO_2 equivalent by multiplying by 44/12, that is, by the ratio between the weight of carbon dioxide (44 atomic mass units) and the atomic weight of carbon (12 atomic mass units). Despite the present study not delving into the origin of the OM found in the salt marsh soils, we consider it plausible that the majority of it originates internally within the lagoon system, as the Venice Lagoon is currently characterized by minimal inputs of sediment from both riverine and marine sources (Carniello et al., 2012; Tognin et al., 2021).

The average carbon accumulation rate estimate from our study ($85 \pm 25 \text{ ton C km}^{-2} \text{ yr}^{-1}$) is lower than current global means (McLeod et al., 2011; Nellesmann et al., 2009), although it falls within the broad range defined by previous estimates, which span from 27 to 273 $\text{ton C km}^{-2} \text{ yr}^{-1}$ (Sifleet et al., 2011).

To better contextualize our results, we examined the difference between estimates of carbon accumulation rate estimates using various time scales and reference intervals in the Venice Lagoon. As expected, we found higher SCD values in the topsoil (5 cm). However, marsh accretion rate estimates show higher short-term estimates in the northern lagoon, where recent accretion rates are higher, and slightly higher long-term estimates in the southern lagoon, where accretion rates have decreased over time (Puppini et al., 2024).

By multiplying the mean C accumulation rate (based on top-5-cm reference interval, $85 \pm 25 \text{ ton C km}^{-2} \text{ yr}^{-1}$) by the total salt marsh area (43 km^2) (Carniello et al., 2009), and converting the mass of carbon into CO_2 equivalents, we estimated that the salt marsh soils of the Venice Lagoon may sequester about 13,436 tons of CO_2 per year. This amount represents about 20% of the annual emissions from waterborne navigation in the city of Venice ($66,000 \text{ ton CO}_2\text{e yr}^{-1}$) or about 17% of the annual local emissions from the aviation system at the Venice Marco Polo Airport ($77,000 \text{ ton CO}_2\text{e yr}^{-1}$) (CIRIS–City Inventory Reporting and Information System–2018) (Figure 13). These findings underscore the critical role of salt marsh ecosystems in mitigating GHG effects.

Carbon sequestration has a monetary value, which can be assessed through the market price of carbon set in carbon offset markets. In the European Emission Trading System (EU ETS), the first-established and largest carbon market globally, the average spot price of emission allowances (EUA) was about 80 euros per ton of CO_2e in 2022, whereas it was about 84 euros per ton of CO_2e in 2023 (<https://www.eex.com/en/market-data/environmental-markets/auction-market>). Based on the average 2022 spot price, the annual CO_2 sequestration value from the salt marshes of the Venice Lagoon (13,436 tons of CO_2e per year) amounts to approximately 1.08 million euros per year, whereas it amounts to approximately 1.12 million euros per year at the 2023 average spot price (Puppini et al., 2024).

It is important to note that EU carbon prices are highly volatile and have rapidly increased since the reform of the EU ETS in 2018 (Directive 2018/410/EU). EUA spot prices undergone a further skyrocket growth starting in 2021, reaching a record high of about 100 euros per ton of CO_2e in February 2023, and they are currently undergoing a slight decrease. The observed increase in EU carbon prices might continue in the future, as a

result of the ever-growing challenge of meeting emission reduction targets. As a result, the monetary values of the annual CO₂ sequestration in the salt marshes of the Venice Lagoon might similarly increase, making policies for marsh preservation and restoration increasingly appealing.

Assuming newly constructed marshes could, over time, achieve carbon sequestration rates comparable to those of older, established marshes, the total sequestration potential could increase proportionally with expanded restoration efforts. In a restoration scenario aimed at recovering salt marsh areas to their historical extent from the early 1900s (approximately 164 km², as estimated by Tommasini et al., 2019), the Venice Lagoon could potentially sequester around 50,000 tons of CO₂ annually (Figure 13). This significant increase underscores the critical role that large-scale marsh restoration could play in enhancing carbon storage capacity and contributing to climate mitigation goals.

Future research is crucial to deepen our understanding of the long-term carbon sequestration dynamics in restored marsh ecosystems. Such efforts are vital to optimizing restoration practices and ensuring their effectiveness in bolstering climate resilience and maintaining ecological health.

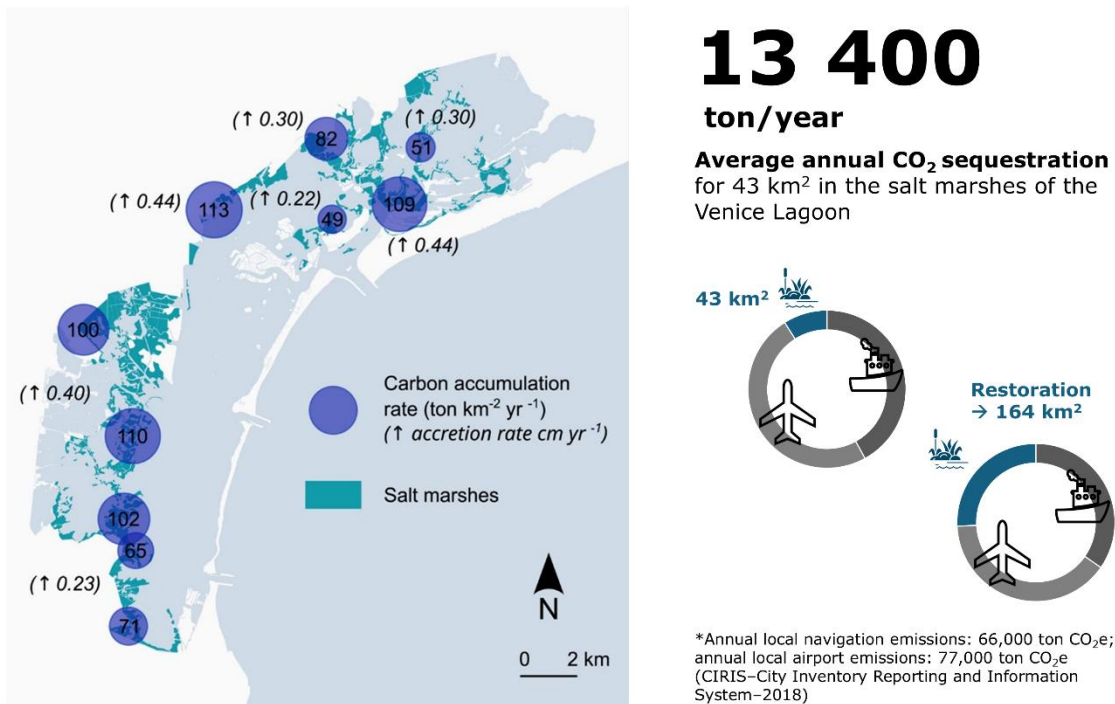


Figure 13. Carbon accumulation and CO₂ sequestration estimate in the salt marshes of the Venice Lagoon (modified from Puppini et al., 2024).

5. Adaptation of coastal defense structures against coastal flooding in the Misa River estuarine system

The adaptation of coastal defense structures to limit sea-driven inundation due to climate change is not a trivial task. Detailed studies are needed to choose the most effective intervention depending on expected forcings, such as the wave climate and sea levels, and site-specific conditions, such as the beach profiles and sediment type.

For example, Marini et al. (2020) compared two adaptation interventions for submerged structures, involving the same volumes and, thus, similar costs: i) the enlargement of the berm width and ii) the increase of the structure height. The authors found that below 0.5 m of sea elevation, the enlargement of the berm width is more effective than the increase of the breakwater elevation, and vice-versa. Further, when the sea level variation is very small, their results showed that elevating the structure is even worse than no adaptation at all. Low-crested structures induce a set-up within the protected zone due to wave overtopping. Such effect is balanced by return flows that globally equal the overtopping discharge. Therefore, small piling-up occurs for well emerged conditions, because the overtopping is limited, or for deeply submerged configurations, since the return flow encounters a low resistance. On the other hand, the greatest water superelevation verifies for almost null freeboard (Martinelli et al., 2006). Several experimental tests confirmed such findings on submerged breakwaters, highlighting that the larger is the structure efficiency in terms of wave transmission, the larger is the piling-up (Lorenzoni et al., 2016). Therefore, if compared to the emerged breakwaters, submerged structures are less indicated for coastal protection purposes, since the piling-up causes a regression of the shoreline and increases the risk of sea ingression on the land.

5.1. Methods

Following the analysis of climate-change driven coastal flooding at the Misa River estuarine site (Senigallia), described in DV1.4.5, a simulation was performed for the 100-years return period scenario with the breakwaters elevation modified to adapt to CC. Emerged breakwaters in the original configuration had an elevation of +1.5 a.s.l. Considering the sum of future SLR and storm surge associated to the 100-years return period scenario, i.e. 1.63 m, such structures became submerged, with an almost null freeboard R_c . The application of the semi-analytical model by Marini et al. (2022) to evaluate the beach recession ΔY depending on the breakwater's freeboard, suggested that the original configuration was the worst in terms of inundation extent. For the model application, we used a beach slope of 1/70, a berm width of 7 m, a sea elevation of 1.63 m, a water depth of 2.3 m at the toe of the structure, a significant wave height of 3.35 m and a period of 9.93 s (wave characteristics at the offshore boundary of the model inner grid). The model assumes a linear slope for the beach, that extends up to +2.5m a.s.l. Figure 14 shows the results of the semi-analytical model in terms of non-dimensional beach recession $\frac{|\Delta Y|}{H_0}$ as a function of R_c . The largest recession is given by a +1.5 m freeboard, that corresponds to the original breakwater elevation. Values of R_c larger than 2 m make the structure emerged in the future scenario, significantly reducing the beach recession.

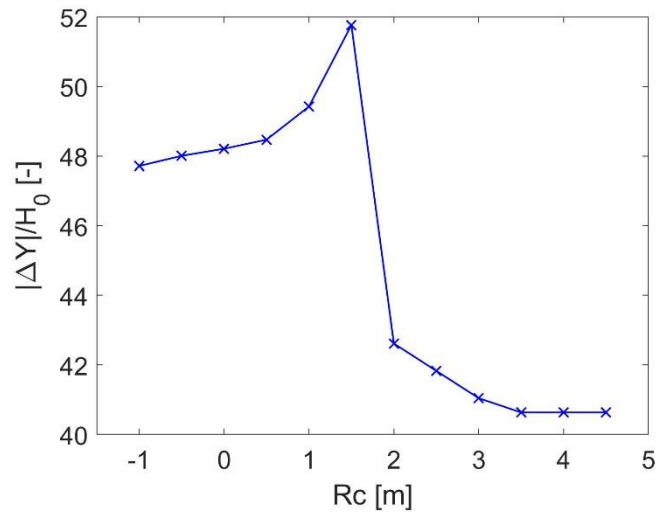


Figure 14. Results of the semi-analytical model by Marini et al. (2022), showing the non-dimensional beach profile recession $\frac{|\Delta Y|}{H_0}$ depending on the breakwater freeboard R_c .

Given the results shown in Figure 1, the breakwater elevation was increased up to +2.5 m a.s.l., which means a freeboard of about +1 m in the future scenario.

5.2. Results

The two inundation perimeters obtained with original and adapted breakwaters are almost superimposed. This is because the largest amount of inundation is caused by the sea superelevation imposed for the 100-years return period scenario (1.63 m). The contribution to inundation given by waves is limited by artificial boundaries, such as roads and houses. Unlike the beach profile considered in the semi-analytical model, the real beach does not extend with a linear slope up to 2.5 m a.s.l. and therefore the real beach recession differs from the computed one. However, the effect of different breakwaters elevations can be observed in terms of differences in water depths in the flooded areas. Figure 15 shows such differences computed between the simulations with the original and adapted breakwaters. The increase of the breakwaters elevation reduces the water depths in the inundated areas up to 20 cm.

Figure 16 and Figure 17 show the comparison in terms of mean water level and maximum wave height for the runs with original and adapted breakwaters. The piling-up due to the almost null freeboard of the former case is well visible in the left panel of Figure 16 and explains the larger water depths obtained with the original configuration. The adapted configuration is also better in terms of wave attenuation, as can be observed in Figure 17, where the reflection of waves due to the emerged structures is also visible (increase of wave height in the region offshore of the breakwaters).

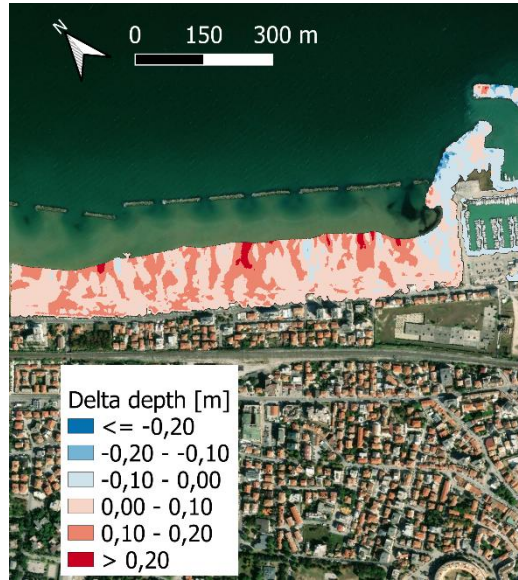


Figure 15. Map of the differences in water depths in the flooded areas behind the breakwaters. The difference was computed between the simulations run with i) original breakwaters and ii) adapted breakwaters.

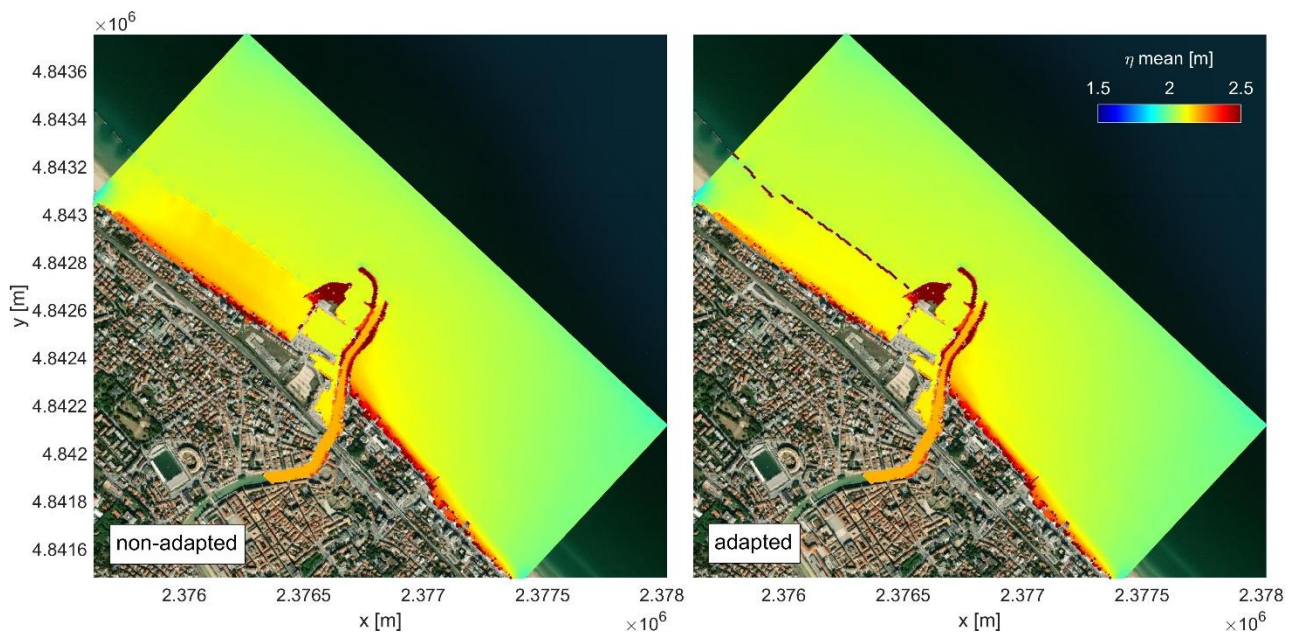


Figure 16. Map of the mean water levels at the sixth hour of the simulations (peak of the simulated storm) run with original breakwaters (left) and adapted breakwaters (right).

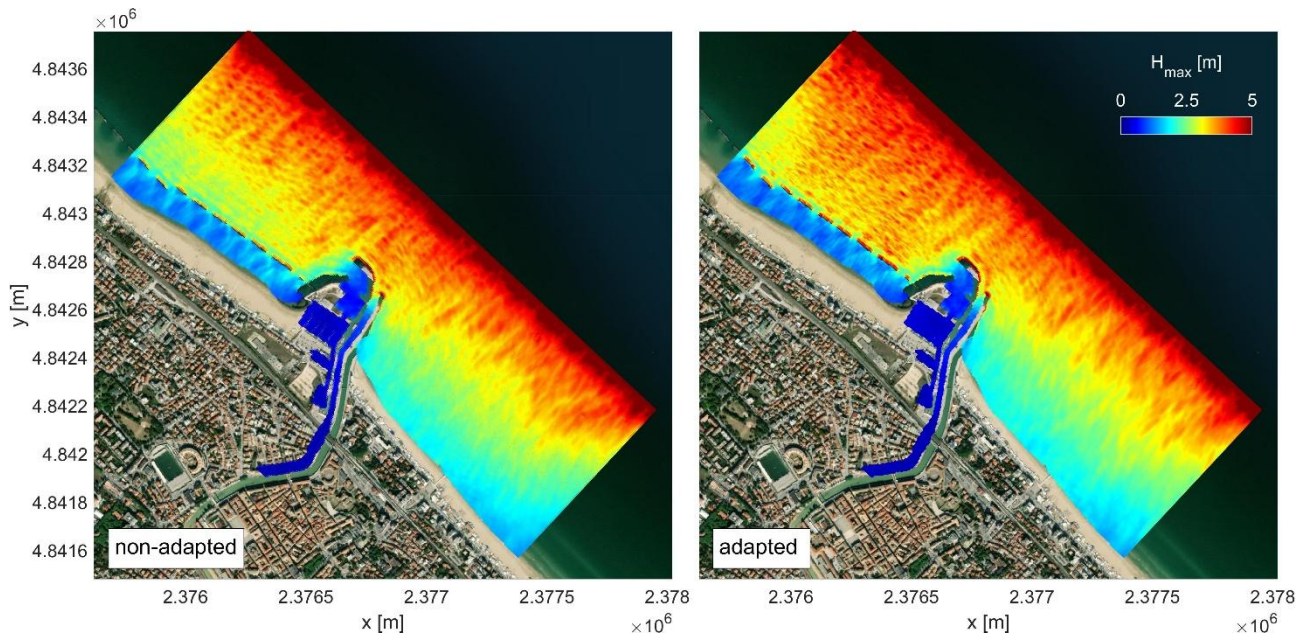


Figure 17. Map of the maximum wave height at the sixth hour of the simulations (peak of the simulated storm) run with original breakwaters (left) and adapted breakwaters (right).

References

- Alves, R. M., Vanaverbeke, J., Bouma, T. J., Guarini, J. M., Vincx, M., & Van Colen, C. (2017). Effects of temporal fluctuation in population processes of intertidal *Lanice conchilega* (Pallas, 1766) aggregations on its ecosystem engineering. *Estuarine, Coastal and Shelf Science*, 188, 88–98.
- Amos, C. L., Umgieser, G., Ferrarin, C., Thompson, C. E. L., Whitehouse, R. J. S., Sutherland, T. F., & Bergamasco, A. (2010). The erosion rates of cohesive sediments in Venice lagoon, Italy. *Continental Shelf Research*, 30(8), 859–870. <https://doi.org/10.1016/j.csr.2009.12.001>
- Barausse, A., Grechi, L., Martinello, N., Musner, T., Smania, D., Zangaglia, A., & Palmeri, L. (2015). An integrated approach to prevent the erosion of salt marshes in the lagoon of Venice. *EQA - International Journal of Environmental Quality*, 18(1), 43–54. <https://doi.org/10.6092/issn.2281-4485/5799>
- Barbier, E. B., Hacker, S. D. S. D., Kennedy, C., Koch, E. W. E. W., Stier, A. C. A. C., & Silliman, B. R. B. R. (2011). The value of estuarine and coastal ecosystem services. *Ecological Monographs*, 81(2), 169–193. <https://doi.org/10.1890/10-1510.1>
- Beck, M. W., Brumbaugh, R. D., Airoidi, L., Carranza, A., Coen, L. D., Crawford, C., Guo, X., et al. (2011). Oyster reefs at risk and recommendations for conservation, restoration, and management. *Bioscience*, 61, 107–116.
- Bellucci, L. G., Frignani, M., Cochran, J. K., Albertazzi, S., Zaggia, L., Cecconi, G., & Hopkins, H. (2007). ²¹⁰Pb and ¹³⁷Cs as chronometers for salt marsh accretion in the Venice Lagoon - links to flooding frequency and climate change. *Journal of Environmental Radioactivity*, 97(2–3), 85–102. <https://doi.org/10.1016/j.jenvrad.2007.03.005>
- Bersoza Hernández, A., Brumbaugh, R. D., Frederick, P., Grizzle, R., Luckenbach, M. W., Peterson, C. H., & Angelini, C. (2018). Restoring the eastern oyster: how much progress has been made in 53 years?. *Frontiers in Ecology and the Environment*, 16, 463–471.
- Biolchi, L. G., Unguendoli, S., Bressan, L., Giambastiani, B. M. S., & Valentini, A. (2022). Ensemble technique application to an XBeach-based coastal Early Warning System for the Northwest Adriatic Sea (Emilia-Romagna region, Italy). *Coastal Engineering*, 173, 104081.
- Bonometto, A., Sfriso, A., Oselladore, F., Ponis, E., Cornello, M., Facca, C., Boscolo, R. (2018). Il trapianto di fanerogame acquatiche come misura per il ripristino delle lagune costiere. *ISPRA, Quaderni – Ricerca marina*, 12/2018, 52.
- Boscolo Brusà, R., Feola, A., Cacciatore, F., Ponis, E., Sfriso, A., Franzoi, P., Lizier, M., Peretti, P., Matticchio, B., Baccetti, N., Volpe, V., Maniero, L., & Bonometto, A. (2022). Conservation actions for restoring the coastal lagoon habitats: Strategy and multidisciplinary approach of LIFE Lagoon Refresh. *Frontiers in Ecology and Evolution*, 10, 979415. <https://doi.org/10.3389/fevo.2022.979415>
- Brambati, A., Carbognin, L., Quaia, T., Teatini, P., & Tosi, L. (2003). The Lagoon of Venice: Geological setting, evolution and land subsidence. *Episodes*, 26(3), 264–265. <https://doi.org/10.18814/epiiugs/2003/v26i3/020>
- Breda, A., Saco, P. M., Sandi, S. G., Saintilan, N., Riccardi, G., & Rodríguez, J. F. (2021). Accretion, retreat and transgression of coastal wetlands experiencing sea-level rise. *Hydrology and Earth System Sciences*, 25(2), 769–786. <https://doi.org/10.5194/hess-25-769-2021>
- Briganti, R., Van der Meer, J. W., Buccino, M., & Calabrese, M. (2003). Wave transmission behind low-crested structures. In *Coastal Structures 2003 - Proceedings of the Conference*, 26–30 August 2003, 580–592.

- Bruschetti, M. (2019). Role of reef-building, ecosystem engineering polychaetes in shallow water ecosystems. *Diversity*, 11, 168.
- Carbognin, L., Teatini, P., & Tosi, L. (2004). Eustacy and land subsidence in the Venice Lagoon at the beginning of the new millennium. *Journal of Marine Systems*, 51(1–4 SPEC. ISS.), 345–353. <https://doi.org/10.1016/j.jmarsys.2004.05.021>
- Carniello, L., D'Alpaos, A., & Defina, A. (2011). Modeling wind waves and tidal flows in shallow micro-tidal basins. *Estuarine, Coastal and Shelf Science*, 92(2), 263–276. <https://doi.org/10.1016/j.ecss.2011.01.001>
- Carniello, L., Defina, A., & D'Alpaos, L. (2009). Morphological evolution of the Venice lagoon: Evidence from the past and trend for the future. *Journal of Geophysical Research: Earth Surface*, 114, F04002. <https://doi.org/10.1029/2008JF001157>
- Carniello, L., Defina, A., & D'Alpaos, L. (2012). Modeling sand-mud transport induced by tidal currents and wind waves in shallow microtidal basins: Application to the Venice Lagoon (Italy). *Estuarine, Coastal and Shelf Science*, 102–103, 105–115. <https://doi.org/10.1016/j.ecss.2012.03.016>
- Carniello, L., Defina, A., Fagherazzi, S., & D'Alpaos, L. (2005). A combined wind wave-tidal model for the Venice lagoon, Italy. *Journal of Geophysical Research: Earth Surface*, 110(4), 1–15. <https://doi.org/10.1029/2004JF000232>
- Carniello, L., Silvestri, S., Marani, M., D'Alpaos, A., Volpe, V., & Defina, A. (2014). Sediment dynamics in shallow tidal basins: In situ observations, satellite retrievals, and numerical modeling in the Venice Lagoon. *Journal of Geophysical Research: Earth Surface*, 119(4), 802–815. <https://doi.org/10.1002/2013JF003015>
- Casadei, I., Gaeta, M. G., & Archetti, R. (2024). Studio di impatto di un reef a ostriche e sabelarie mediante modellazione con XBeach. *Atti del XXXIX Convegno Nazionale di Idraulica e Costruzioni Idrauliche*, Parma, 15–18 Settembre 2024.
- Chmura, G. L., Anisfeld, S. C., Cahoon, D. R. D. R., & Lynch, J. C. J. C. (2003). Global carbon sequestration in tidal, saline wetland soils. *Global Biogeochemical Cycles*, 17(4), 22–1. <https://doi.org/10.1029/2002GB001917>
- Clarkson, B. R., Ausseil, A. E., & Gerbeaux, P. (2013). Wetland ecosystem services. In J. R. Dymond (Ed.), *Ecosystem services in New Zealand—conditions and trends*.
- Colsoul, B., Pouvreau, S., Di Poi, C., Pouil, S., Merk, V., Peter, C., Boersma, M., & Pogoda, B. (2020). Addressing critical limitations of oyster (*Ostrea edulis*) restoration: Identification of nature-based substrates for hatchery production and recruitment in the field. *Aquatic Conservation: Marine and Freshwater Ecosystems*, 30, 2101–2115.
- Costanza, R., D'Arge, R., De Groot, R., Farber, S., Grasso, M., Hannon, B., et al. (1997). The value of the world's ecosystem services and natural capital. *Nature*, 387(6630), 253–260. <https://doi.org/10.1038/387253a0>
- Craft, C. B., Seneca, E. D., & Broome, S. W. (1991). Loss on ignition and Kjeldahl digestion for estimating organic carbon and total nitrogen in estuarine marsh soils: Calibration with dry combustion. *Estuaries*, 14(2), 175–179. <https://doi.org/10.2307/1351691>
- D'Alpaos, A. (2011). The mutual influence of biotic and abiotic components on the long-term ecomorphodynamic evolution of salt-marsh ecosystems. *Geomorphology*, 126(3–4), 269–278. <https://doi.org/10.1016/j.geomorph.2010.04.027>

- D'Alpaos, A., & Marani, M. (2016). Reading the signatures of biologic-geomorphic feedbacks in salt-marsh landscapes. *Advances in Water Resources*, 93, 265–275. <https://doi.org/10.1016/j.advwatres.2015.09.004>
- D'Alpaos, A., Carniello, L., & Rinaldo, A. (2013). Statistical mechanics of wind wave-induced erosion in shallow tidal basins: Inferences from the Venice Lagoon. *Geophysical Research Letters*, 40(13), 3402–3407. <https://doi.org/10.1002/grl.50666>
- D'Alpaos, A., Lanzoni, S., Marani, M., & Rinaldo, A. (2009). On the O'Brien-Jarrett-Marchi law. *Rendiconti Lincei*, 20(3), 225–236. <https://doi.org/10.1007/s12210-009-0052-x>
- D'Alpaos, L. (2010). Fatti e misfatti di idraulica lagunare. La laguna di Venezia dalla diversione dei fiumi alle nuove opere delle bocche di porto. In L. D'Alpaos (Ed.), *Istituto Veneto di Scienze, Lettere e Arti*, Vol. 1999. Venice: Istituto Veneto di Scienze, Lettere ed Arti.
- D'Angremond, K., Van der Meer, J. W., & De Jong, R. J. (1996). Wave transmission at low crested structures. In *Proc. 25th Int. Conf. on Coastal Engineering* (pp. 3305–3318). ASCE.
- Davies, B. R., Stuart, V., & De Villiers, M. (1989). The filtration activity of a serpulid polychaete population (*Ficopomatus enigmaticus* (Fauvel)) and its effects on water quality in a coastal marina. *Estuarine, Coastal and Shelf Science*, 29, 613–620.
- Day, J. W., Britsch, L. D., Hawes, S. R., Shaffer, G. P., Reed, D. J., & Cahoon, D. (2000). Pattern and process of land loss in the Mississippi Delta: A spatial and temporal analysis of wetland habitat change. *Estuaries*, 23(4), 425–438. <https://doi.org/10.2307/1353136>
- Defina, A. (2000). Two-dimensional shallow flow equations for partially dry areas. *Water Resources Research*, 36(11), 3251–3264. <https://doi.org/10.1029/2000WR900167>
- DeLaune, R. D., & Pezeshki, S. R. (2003). The role of soil organic carbon in maintaining surface elevation in rapidly subsiding U.S. Gulf of Mexico coastal marshes. *Water, Air, and Soil Pollution: Focus*, 3(1), 167–179. <https://doi.org/10.1023/A:1022136328105>
- Duarte, C. M., Middelburg, J. J., & Caraco, N. (2005). Major role of marine vegetation on the oceanic carbon cycle. *Biogeosciences*, 2(1), 1–8. <https://doi.org/10.5194/bg-2-1-2005>
- Eggermont, H., Balian, E., Azevedo, J. M. N., Beumer, V., Brodin, T., Claudet, J., ... & Le Roux, X. (2015). Nature-based solutions: new influence for environmental management and research in Europe. *GAIA-Ecological Perspectives for Science and Society*, 24(4), 243–248.
- Feola, A., Ponis, E., Cornello, M., Boscolo Brusà, R., Cacciatore, F., Oselladore, F., et al. (2022). An integrated approach for evaluating the restoration of the salinity gradient in transitional waters: Monitoring and numerical modeling in the Life Lagoon Refresh case study. *Environments*, 9(31). <https://doi.org/10.3390/environments9030031>
- Ferrarin, C., Tomasin, A., Bajo, M., Petrizzo, A., & Umgiesser, G. (2015). Tidal changes in a heavily modified coastal wetland. *Continental Shelf Research*, 101, 22–33. <https://doi.org/10.1016/j.csr.2015.04.002>
- Finotello, A., Canestrelli, A., Carniello, L., Ghinassi, M., & D'Alpaos, A. (2019). Tidal flow asymmetry and discharge of lateral tributaries drive the evolution of a microtidal meander in the Venice Lagoon (Italy). *Journal of Geophysical Research: Earth Surface*, 124(12), 3043–3066. <https://doi.org/10.1029/2019JF005193>
- Finotello, A., Capperucci, R. M., Bartholomä, A., D'Alpaos, A., & Ghinassi, M. (2022). Morpho-sedimentary evolution of a microtidal meandering channel driven by 130 years of natural and anthropogenic modifications of the Venice Lagoon (Italy). *Earth Surface Processes and Landforms*, 47(10), 2580–2596. <https://doi.org/10.1002/esp.5396>

- Finotello, A., D'Alpaos, A., Bogoni, M., Ghinassi, M., & Lanzoni, S. (2020). Remotely-sensed planform morphologies reveal fluvial and tidal nature of meandering channels. *Scientific Reports*, 10(1), 1–13. <https://doi.org/10.1038/s41598-019-56992-w>
- Finotello, A., Tognin, D., Carniello, L., Ghinassi, M., Bertuzzo, E., & D'Alpaos, A. (2020). Hydrodynamic feedbacks of salt-marsh loss in the shallow microtidal back-barrier lagoon of Venice (Italy). *Water Resources Research*, 59(32). <https://doi.org/10.1029/2022WR032881>
- Fitzgerald, D. M., & Hughes, Z. J. (2019). Marsh processes and their response to climate change and sea-level rise. *Annual Review of Earth and Planetary Sciences*, 47(1), 481–517. <https://doi.org/10.1146/annurev-earth-082517-010255>
- Gatto, P., & Carbognin, L. (1981). The lagoon of Venice: Natural environmental trend and man-induced modification. *Hydrological Sciences Bulletin*, 26(4), 379–391. <https://doi.org/10.1080/02626668109490902>
- Gedan, K. B., Silliman, B. R., & Bertness, M. D. (2009). Centuries of human-driven change in salt marsh ecosystems. *Annual Review of Marine Science*, 1, 117–141. <https://doi.org/10.1146/annurev.marine.010908.163930>
- Ghezzi, M., Guerzoni, S., Cucco, A., & Umgiesser, G. (2010). Changes in Venice Lagoon dynamics due to construction of mobile barriers. *Coastal Engineering*, 57(7), 694–708. <https://doi.org/10.1016/j.coastaleng.2010.02.009>
- Grabowski, J. H., Brumbaugh, R. D., Conrad, R. F., Keeler, A. G., Opaluch, J. J., Peterson, C. H., Smyth, A., et al. (2012). Economic valuation of ecosystem services provided by oyster reefs. *Bioscience*, 62, 900–909.
- Howard, J., Hoyt, S., Isensee, K., Telszewski, M., & Pidgeon, E. (2014). Coastal blue carbon: Methods for assessing carbon stocks and emissions factors in mangroves, tidal salt marshes, and seagrasses (J. Howard, S. Hoyt, K. Isensee, M. Telszewski, & E. Pidgeon, Eds.). Arlington, Virginia, USA: Conservation International, Intergovernmental Oceanographic Commission of UNESCO, International Union for Conservation of Nature.
- Hudson, R., Kenworth, J., & Best, M. (2021). *Saltmarsh restoration handbook*.
- Jarrett, J. T. (1976). Tidal prism–inlet area relationships. *Journal of Waterways and Harbors*, 95(General Investigation of Tidal Inlets, Report 3), 55.
- Kolker, A. S., Goodbred, S. L., Hameed, S., & Cochran, J. K. (2009). High-resolution records of the response of coastal wetland systems to long-term and short-term sea-level variability. *Estuarine, Coastal and Shelf Science*, 84(4), 493–508. <https://doi.org/10.1016/j.ecss.2009.06.030>
- Kroeger, T. (2012). Dollars and sense: Economic benefits and impacts from two oyster reef restoration projects in the northern Gulf of Mexico. *The Nature Conservancy*, 101.
- Leonardi, N., Defne, Z., Ganju, N. K., & Fagherazzi, S. (2016). Salt marsh erosion rates and boundary features in a shallow bay. *Journal of Geophysical Research: Earth Surface*, 121(10), 1861–1875. <https://doi.org/10.1002/2016JF003975>
- Lesser, G. R., Roelvink, J. A., van Kester, J. A. T. M., & Stelling, G. S. (2004). Development and validation of a three-dimensional morphological model. *Coastal Engineering*, 51(8–9), 883–915. <https://doi.org/10.1016/j.coastaleng.2004.07.014>
- Lorenzoni, C., Postacchini, M., Brocchini, M., & Mancinelli, A. (2016). Experimental study of the short-term efficiency of different breakwater configurations on beach protection. *Journal of Ocean Engineering and Marine Energy*, 2(2), 195–210. <https://doi.org/10.1007/s40722-016-0051-9>

- Macreadie, P. I., Anton, A., Raven, J. A., Beaumont, N., Connolly, R. M., Friess, D. A., et al. (2019). The future of Blue Carbon science. *Nature Communications*, 10(1), 1–13. <https://doi.org/10.1038/s41467-019-11693-w>
- Marani, M., D'Alpaos, A., Lanzoni, S., & Santalucia, M. (2011). Understanding and predicting wave erosion of marsh edges. *Geophysical Research Letters*, 38(21), 1–5. <https://doi.org/10.1029/2011GL048995>
- Marchand, Y., & Cazoulat, R. (2003). Biological reef survey using spot satellite data classification by cellular automata method—Bay of Mont Saint-Michel (France). *Computers & Geosciences*, 29, 413–421.
- Marini, F., Corvaro, S., Rocchi, S., Lorenzoni, C., & Mancinelli, A. (2022). Semi-analytical model for the evaluation of shoreline recession due to waves and sea level rise. *Water*, 14(8), 1305. <https://doi.org/10.3390/w14081305>
- Marini, F., Mancinelli, A., Corvaro, S., Rocchi, S., & Lorenzoni, C. (2020). Coastal submerged structures adaptation to sea level rise over different beach profiles. *Italian Journal of Engineering Geology and Environment*, 87-98. <https://doi.org/10.4408/IJEGE.2020-01.S-10>
- Mariotti, G., & Fagherazzi, S. (2010). A numerical model for the coupled long-term evolution of salt marshes and tidal flats. *Journal of Geophysical Research: Earth Surface*, 115(1). <https://doi.org/10.1029/2009JF001326>
- Mariotti, G., & Fagherazzi, S. (2013). Wind waves on a mudflat: The influence of fetch and depth on bed shear stresses. *Continental Shelf Research*, 60, S99-S110. <https://doi.org/10.1016/j.csr.2012.03.001>
- Martin, E. G., Costa, M. M., & Mániz, K. S. (2020). An operationalized classification of nature-based solutions for water-related hazards: From theory to practice. *Ecological Economics*, 167, 106460. <https://doi.org/10.1016/j.ecolecon.2019.106460>
- Martinelli, L., Zanuttigh, B., & Lamberti, A. (2006). Hydrodynamic and morphodynamic response of isolated and multiple low crested structures: Experiments and simulations. *Coastal Engineering*, 53(4), 363-379. <https://doi.org/10.1016/j.coastaleng.2005.10.018>
- Matticchio, B., Carniello, L., Canesso, D., Ziggliotto, E., & Cordella, M. (2017). Recent changes in tidal propagation in the Venice Lagoon: Effects of changes in the inlet structure. In L. D'Alpaos (Ed.), *Commissione di studio sui problemi di Venezia, Volume III: La laguna di Venezia e le nuove opere alle bocche* (pp. 157–183). Venice: Istituto Veneto di Scienze, Lettere ed Arti.
- McLeod, E., Chmura, G. L., Bouillon, S., Salm, R., Björk, M., Duarte, C. M., et al. (2011). A blueprint for blue carbon: Toward an improved understanding of the role of vegetated coastal habitats in sequestering CO₂. *Frontiers in Ecology and the Environment*, 9(10), 552–560. <https://doi.org/10.1890/110004>
- McQuaid, S., Kooijman, E., Rizzi, D., Andersson, T., & Schanté, J. (2022). *The vital role of nature-based solutions in a nature-positive economy*. Publications Office of the European Union, 2022.
- Mehta, A. J., Hayter, E. J., Parker, W. R., Krone, R. B., & Teeter, A. M. (1989). Cohesive sediment transport. I: Process description. *Journal of Hydraulic Engineering*, 115(8), 1076–1093. [https://doi.org/10.1061/\(ASCE\)0733-9429\(1989\)115:8\(1076\)](https://doi.org/10.1061/(ASCE)0733-9429(1989)115:8(1076))
- Mel, R. A., Viero, D. P., Carniello, L., Defina, A., & D'Alpaos, L. (2021). The first operations of Mo.S.E. system to prevent the flooding of Venice: Insights on the hydrodynamics of a regulated lagoon. *Estuarine, Coastal and Shelf Science*, 261, 107547. <https://doi.org/10.1016/j.ecss.2021.107547>
- Mitsch, W. J., & Gossilink, J. G. (2000). The value of wetlands: Importance of scale and landscape setting. *Ecological Economics*, 35(1), 25–33. [https://doi.org/10.1016/S0921-8009\(00\)00165-8](https://doi.org/10.1016/S0921-8009(00)00165-8)

- Möller, I., Spencer, T., French, J. R., Leggett, D. J., & Dixon, M. (1999). Wave transformation over salt marshes: A field and numerical modelling study from north Norfolk, England. *Estuarine, Coastal and Shelf Science*, 49(3), 411–426. <https://doi.org/10.1006/ecss.1999.0509>
- Mudd, S. M. (2011). The life and death of salt marshes in response to anthropogenic disturbance of sediment supply. *Geology*, 39(5), 511–512. <https://doi.org/10.1130/focus052011.1>
- Nascimbeni, P. (Ed). (2007). *Proposte per la progettazione di interventi di ingegneria naturalistica funzionali alla salvaguardia della morfologia della laguna di Venezia: manuale tecnico*. Consorzio Venezia Nuova; Magistrato alle Acque, Noventa Padovana: Grafiche Leone, Venice.
- Nellemann, C., Corcoran, E., Duarte, C. M., Valdés, L., De Young, C., Fonseca, L., & Grimsditch, G. (2009). *Blue carbon: A Rapid Response Assessment*. (C. Nellemann, E. Corcoran, C. M. Duarte, L. Valdés, C. De Young, L. Fonseca, & G. Grimsditch, Eds.), Environment. UN Environment, GRID-Arendal. Retrieved from http://www.grida.no/files/publications/blue-carbon/BlueCarbon_screen.pdf
- Parker, G., Garcia, M., Fukushima, Y., & Yu, W. (1987). Experiments on turbidity currents over an erodible bed. *Journal of Hydraulic Research*, 25, 123–147. <https://doi.org/10.1080/00221688709499292>
- Perricone, V., Mutalipassi, M., Mele, A., Buono, M., Vicinanza, D., & Contestabile, P. (2023). Nature-based and bioinspired solutions for coastal protection: An overview among key ecosystems and a promising pathway for new functional and sustainable designs. *ICES Journal of Marine Science*, 80(5), 1218–1239. <https://doi.org/10.1093/icesjms/fsad080>
- Pranzini, E., Wetzel, L., & Williams, A. T. (2015). Aspects of coastal erosion and protection in Europe. *Journal of Coastal Conservation*, 19, 445–459. <https://doi.org/10.1007/s11852-015-0399-3>
- Preston, J., Gamble, C., Debney, A., Helmer, L., Hancock, B., & Zu Ermgassen, P. (2020). *European native oyster habitat restoration handbook – UK & Ireland*. The Zoological Society of London, UK, London, UK. ISBN 978-0-900881-80-0.
- Puppin, A., Tognin, D., Paccagnella, M., Zancato, M., Ghinassi, M., D'Alpaos, C., et al. (2024). Blue carbon assessment in the salt marshes of the Venice Lagoon: Dimensions, variability and influence of storm-surge regulation. *Earth's Future*, 12(10), 1–14. <https://doi.org/10.1029/2024EF004715>
- Quintana, X., Boix, D., Gascón, S., Sala, J., & Comín, F. A. (2018). Management and restoration of Mediterranean coastal lagoons in Europe. *Càtedra d'Ecosistemes Litorals Mediterranis, Parc Natural del Montgrí, les Illes Medes i el Baix Ter, Museu de la Mediterrània*.
- Ratliff, K. M., Braswell, A. E., & Marani, M. (2015). Spatial response of coastal marshes to increased atmospheric CO₂. *Proceedings of the National Academy of Sciences of the United States of America*, 112(51), 15580–15584. <https://doi.org/10.1073/pnas.1516286112>
- Roner, M., D'Alpaos, A., Ghinassi, M., Marani, M., Silvestri, S., Franceschinis, E., & Realdon, N. (2016). Spatial variation of salt-marsh organic and inorganic deposition and organic carbon accumulation: Inferences from the Venice lagoon, Italy. *Advances in Water Resources*, 93, 276–287. <https://doi.org/10.1016/j.advwatres.2015.11.011>
- Ruol, P., Favaretto, C., Volpato, M., & Martinelli, L. (2020). Flooding of Piazza San Marco (Venice): Physical model tests to evaluate the overtopping discharge. *Water (Switzerland)*, 12(2), 427. <https://doi.org/10.3390/w12020427>
- Scapin, L., Zucchetto, M., Facca, C., Sfriso, A., & Franzoi, P. (2016). Using fish assemblage to identify success criteria for seagrass habitat restoration. *Web Ecology*, 16, 33–36. <https://doi.org/10.5194/we-16-33-2016>

- Sfriso, A., Buosi, A., Tomio, Y., Juhmani, A.-S., Facca, C., Wolf, M., et al. (2021). Environmental restoration by aquatic angiosperm transplants in transitional water systems: The Venice Lagoon as a case study. *Science of the Total Environment*, 795, 148859. <https://doi.org/10.1016/j.scitotenv.2021.148859>
- Sifleet, S., Pendleton, L., & Murray, B. C. (2011). State of the science on coastal blue carbon: A summary for policy makers. Nicholas Institute for Environmental Policy Solutions. Retrieved from <http://scholar.google.com/scholar?hl=en&btnG=Search&q=intitle:State+of+the+Science+on+Coastal+Blue+Carbon+A+Summary+for+Policy+Makers#0>
- Silvestri, S. (2018). Anthropogenic modifications can significantly influence the local mean sea level and affect the survival of salt marshes in shallow tidal systems. *Journal of Geophysical Research: Earth Surface*, 996–1012. <https://doi.org/10.1029/2017JF004503>
- Tagliapietra, D., Baldan, D., Barausse, A., Buosi, A., Curiel, D., Guarneri, I., et al. (2018). Protecting and restoring the salt marshes and seagrasses in the lagoon of Venice. In X. D. Quintana, D. Boix, S. Gascón, & J. Sala (Eds.), *Management and Restoration of Mediterranean Coastal Lagoons in Europe*. Venice, Italy: Càtedra d'Ecosistemes Litorals Mediterrànies i LIFE Pletera. Retrieved from http://lifepletera.com/wp-content/uploads/2019/02/Recerca_i_Territori_10_ENG_MdM_web.pdf
- Tagliapietra, D., Sigovini, M., & Ghirardini, A. (2009). A review of terms and definitions to categorize estuaries, lagoons, and associated environments. *Marine and Freshwater Research*, 60(6), 497–509.
- Temmerman, S., Bouma, T. J., Govers, G., Wang, Z. B., De Vries, M. B., & Herman, P. M. J. (2005). Impact of vegetation on flow routing and sedimentation patterns: Three-dimensional modeling for a tidal marsh. *Journal of Geophysical Research: Earth Surface*, 110(4), 1–18. <https://doi.org/10.1029/2005JF000301>
- Tognin, D. (2022). Natural and anthropogenic drivers of erosional and depositional dynamics in shallow tidal systems (PhD thesis).
- Tognin, D., D'Alpaos, A., Marani, M., & Carniello, L. (2021). Marsh resilience to sea-level rise reduced by storm-surge barriers in the Venice Lagoon. *Nature Geoscience*, 14(12), 906–911. <https://doi.org/10.1038/s41561-021-00853-7>
- Tognin, D., Finotello, A., D'Alpaos, A., Viero, D. P., Pivato, M., Mel, R. A., et al. (2022). Loss of geomorphic diversity in shallow tidal embayments promoted by storm-surge barriers. *Science Advances*, 8(13), eabm8446. <https://doi.org/10.1126/sciadv.abm8446>
- Tomasin, A. (1974). Recent changes in the tidal regime in Venice. *Rivista Italiana Geofisica*, 23(5/6), 275–278.
- Tommasini, L., Carniello, L., Ghinassi, M., Roner, M., & D'Alpaos, A. (2019). Changes in the wind-wave field and related salt-marsh lateral erosion: Inferences from the evolution of the Venice Lagoon in the last four centuries. *Earth Surface Processes and Landforms*. <https://doi.org/10.1002/esp.4599>
- Unguendoli, S., Biolchi, L. G., Aguzzi, M., Pillai, U. P. A., Alessandri, J., & Valentini, A. (2023). A modeling application of integrated nature-based solutions (NBS) for coastal erosion and flooding mitigation in the Emilia-Romagna coastline (Northeast Italy). *Science of The Total Environment*, 867, 161357. <https://doi.org/10.1016/j.scitotenv.2023.161357>
- Valle-Levinson, A., Marani, M., Carniello, L., D'Alpaos, A., & Lanzoni, S. (2021). Astronomic link to anomalously high mean sea level in the northern Adriatic Sea. *Estuarine, Coastal and Shelf Science*, 257, 107418. <https://doi.org/10.1016/j.ecss.2021.107418>
- Van Ledden, M., Wang, Z. B., Winterwerp, H., & De Vriend, H. (2004). Sand-mud morphodynamics in a short tidal basin. *Ocean Dynamics*, 54(3–4), 385–391. <https://doi.org/10.1007/s10236-003-0050-y>

- van Rijn, L. C. (1984). Sediment Transport. Part I: Bed load transport. *Journal of Hydraulic Engineering*, 110(10), 1431–1456.
- Viero, D. P., & Defina, A. (2016). Water age, exposure time, and local flushing time in semi-enclosed, tidal basins with negligible freshwater inflow. *Journal of Marine Systems*, 156, 16–29. <https://doi.org/10.1016/j.jmarsys.2015.11.006>
- Volpe, V. (2012). La gestione dei sedimenti nella laguna di Venezia: Le previsioni dell' aggiornamento del piano per il recupero morfologico e ambientale della laguna di Venezia. Workshop: “La competitività dei porti: la gestione dei sedimenti” - 8 Marzo 2012. Retrieved from <https://www.slideshare.net/eambiente/volpe-gestionesedimenti-piano-morfologicoadp8marzo2012>
- Woodward, R. T., & Wui, Y. S. (2001). The economic value of wetland services: A meta-analysis. *Ecological Economics*, 37(2), 257–270.
- Yang, Y., Sui, T., Wang, G., Zhang, C., Chen, P., Li, Y., Zeng, J., & Aidoo, R. (2023). Investigations on the shallow water wave attenuation over continuous porous oyster reef-like structure. *Ocean Engineering*, 287(Part 2), 115307. <https://doi.org/10.1016/j.oceaneng.2023.115307>
- Young, I. R., & Verhagen, L. A. (1996). The growth of fetch limited waves in water of finite depth. Part 1. Total energy and peak frequency. *Coastal Engineering*, 29(1–2), 47–78. [https://doi.org/10.1016/S0378-3839\(96\)00006-3](https://doi.org/10.1016/S0378-3839(96)00006-3)
- Ysebaert, T., Walles, B., Haner, J., & Hancock, B. (2019). Habitat modification and coastal protection by ecosystem-engineering reef-building bivalves. In A. C. Smaal, J. G. Ferreira, J. Grant, J. K. Petersen, & Ø. Strand (Eds.), *Goods and Services of Marine Bivalves* (pp. 253–273). Springer International Publishing, Cham.
- Zanchettin, D., Bruni, S., Raicich, F., Lionello, P., Adloff, F., Androsov, A., et al. (2021). Sea-level rise in Venice: Historic and future trends (review article). *Natural Hazards and Earth System Sciences*, 21(8), 2643–2678. <https://doi.org/10.5194/nhess-21-2643-2021>
- Zanin, G. M., Muwafu, S. P., & Costa, M. M. (2024). Nature-based solutions for coastal risk management in the Mediterranean basin: A literature review. *Journal of Environmental Management*, 356, 120667. <https://doi.org/10.1016/j.jenvman.2024.120667>
- Zarzuelo, C., López-Ruiz, A., D'Alpaos, A., Carniello, L., & Ortega-Sánchez, M. (2018). Assessing the morphodynamic response of human-altered tidal embayments. *Geomorphology*, 320, 127–141. <https://doi.org/10.1016/j.geomorph.2018.08.014>
- Zecchin, M., Baradello, L., Brancolini, G., Donda, F., Rizzetto, F., & Tosi, L. (2008). Sequence stratigraphy based on high-resolution seismic profiles in the late Pleistocene and Holocene deposits of the Venice area. *Marine Geology*, 253(3–4), 185–198. <https://doi.org/10.1016/j.margeo.2008.05.010>